MAGIC
Major Atmospheric
Gamma Imaging
Cerenkov Telescopes

Fermi
Gamma-ray
Space Telescope

A multi-wavelength view of the most extreme X-ray flare from Mrk 501

Josefa Becerra González
on behalf of MAGIC, Fermi-LAT collaborations and MWL collaborators
Instituto de Astrofísica de Canarias
jbecerra@iac.es

co-Is: D. Paneque, F. Tavecchio, K. Noda, K. Ishio

MWL Collaborators: E. Linfors, M. Perri, D. Dorner, C. Wendel, K. Mannheim ++

WANTED

MRK 501

FLARING OR QUIESCENT
FOR JETS AND EBL STUDIES

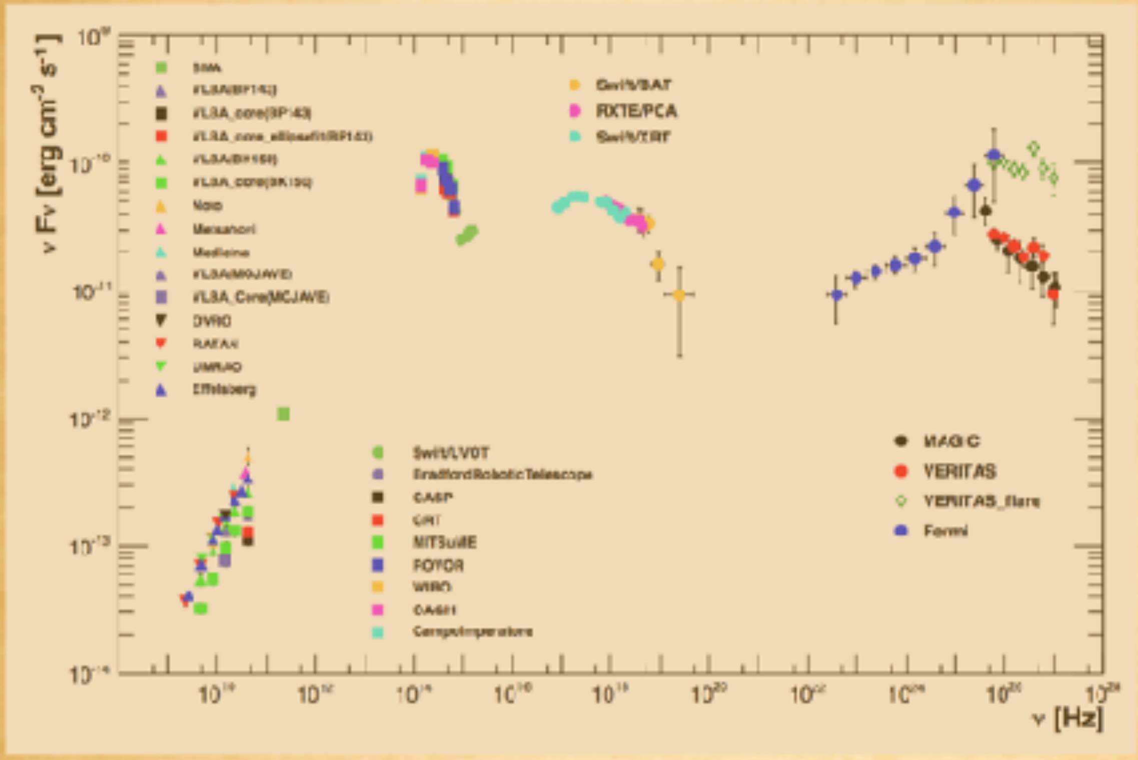

MWL STUDIES REWARDED

WANTED

MRK 501

FLARING OR QUIESCENT
FOR JETS AND EBL STUDIES

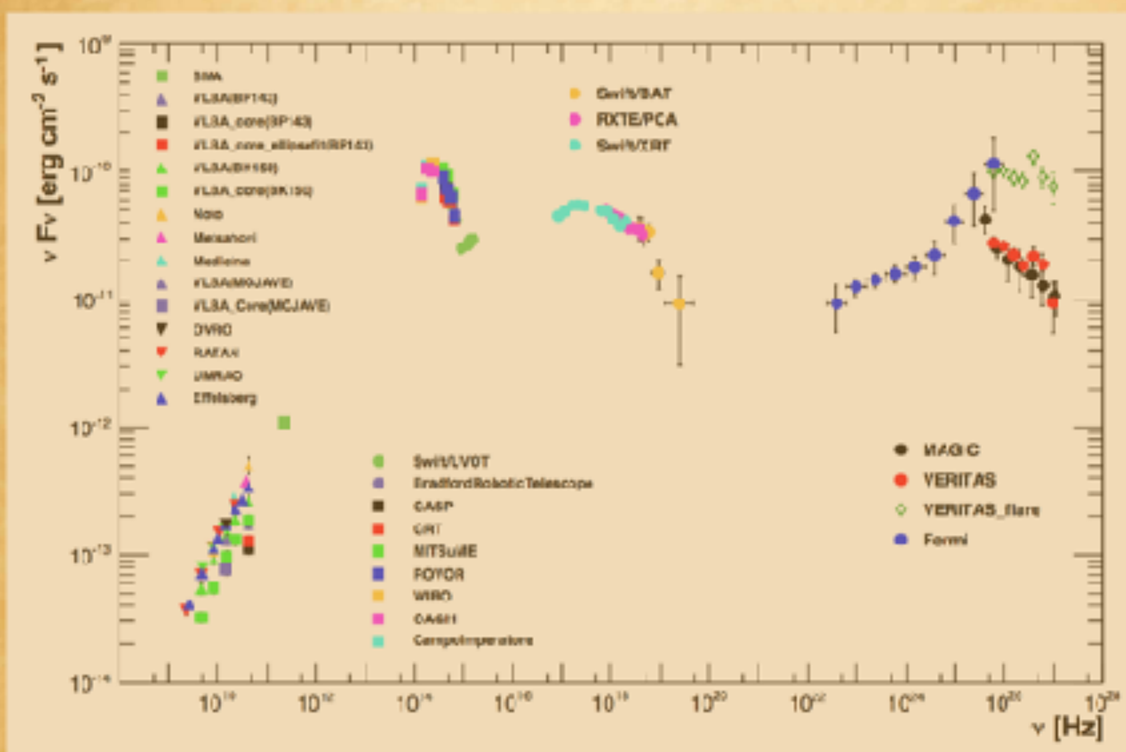

MWL STUDIES REWARDED

Mrk 501:

high-peaked BL Lac at z=0.03
a famous TeV emitter

WANTED

MRK 501

FLARING OR QUIESCENT FOR JETS AND EBL STUDIES

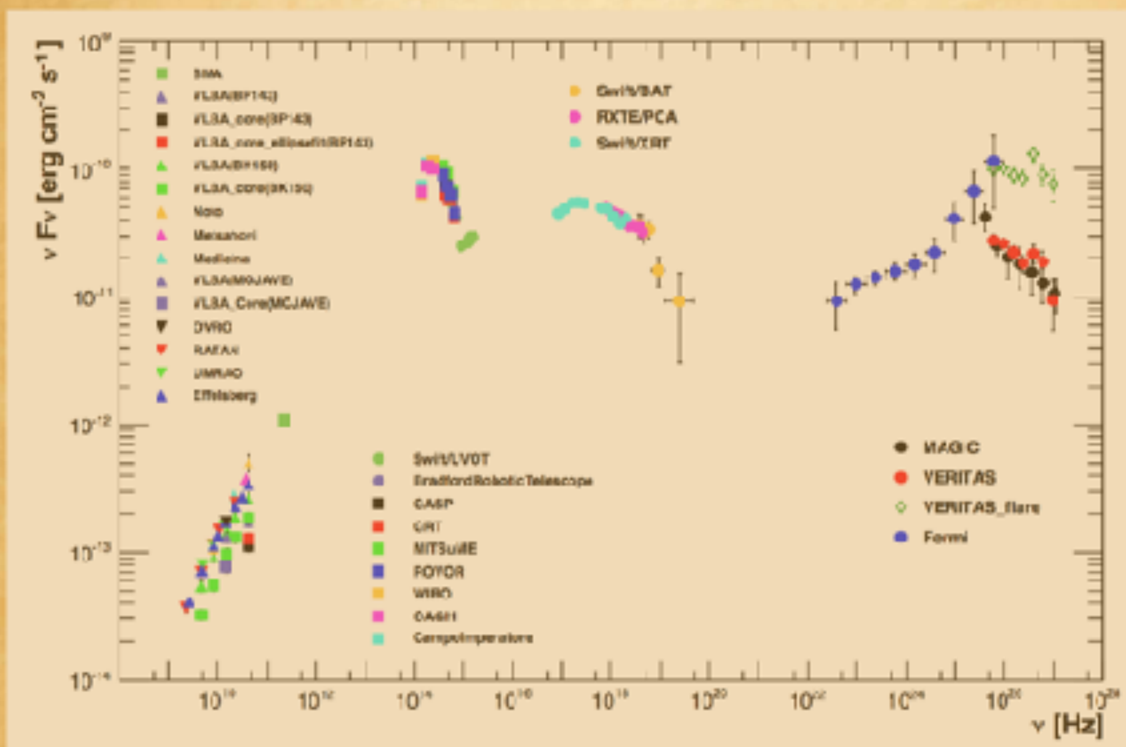

MWL STUDIES REWARDED

Mrk 501:

high-peaked BL Lac at z=0.03
a famous TeV emitter

Its persistent TeV emission during flaring and quiescent phases makes this blazar an excellent candidate for detailed multi-wavelength studies

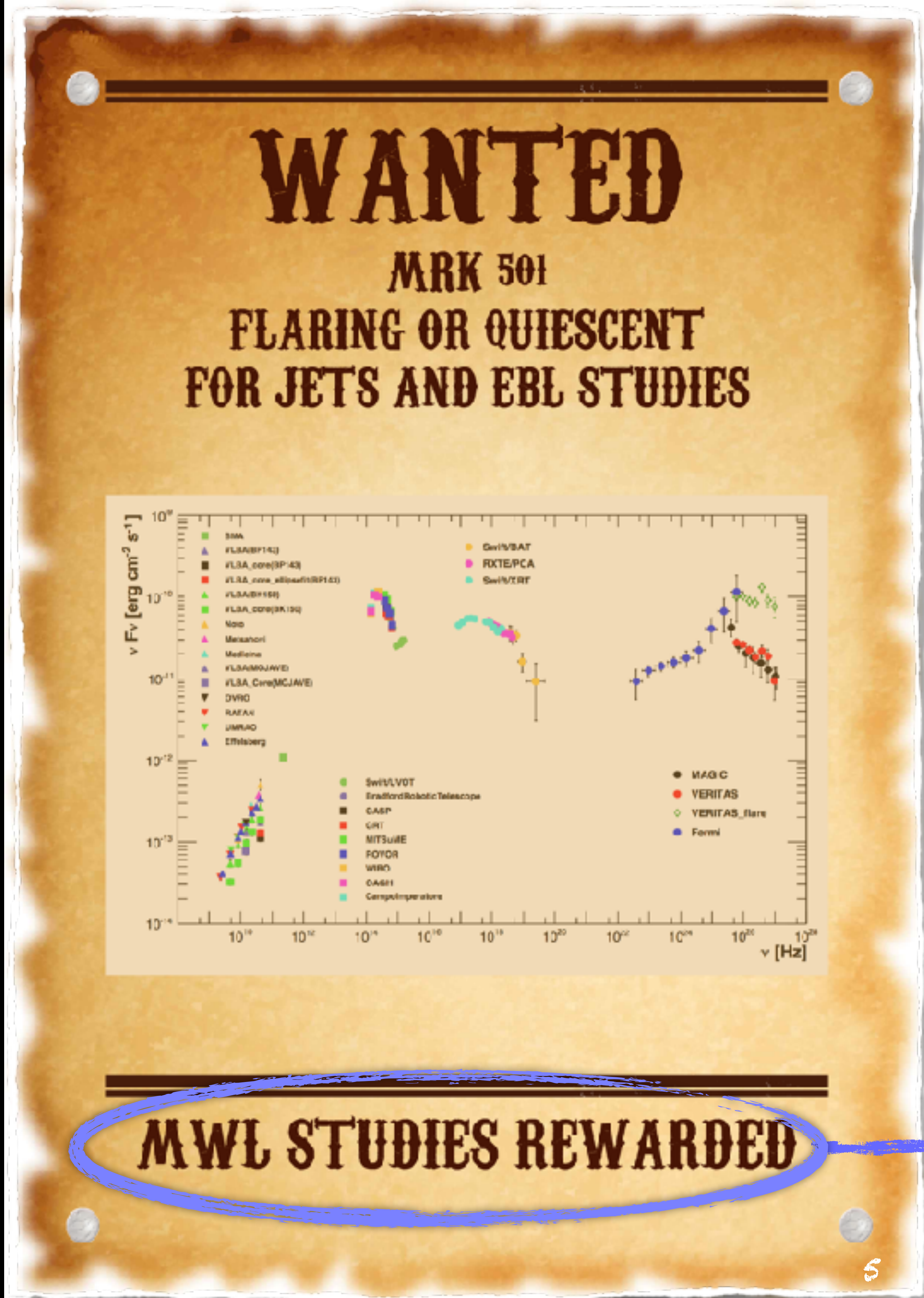

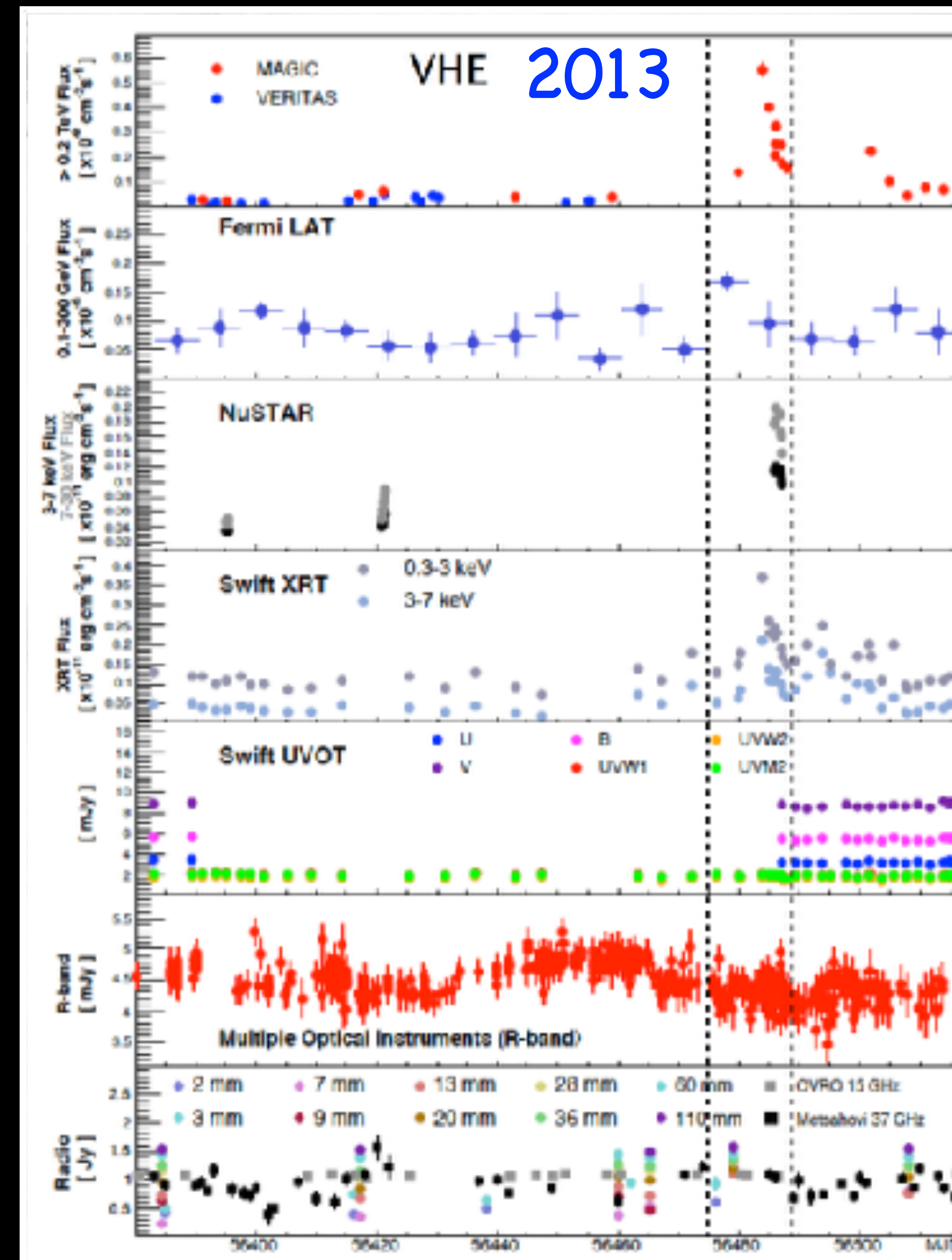

Furnis et al., 2015, ApJ **812,** 65

Multi-wavelength (MWL) variability in different timescales down to minutes. Extensive MWL campaigns are organized including radio to gamma-ray observations.

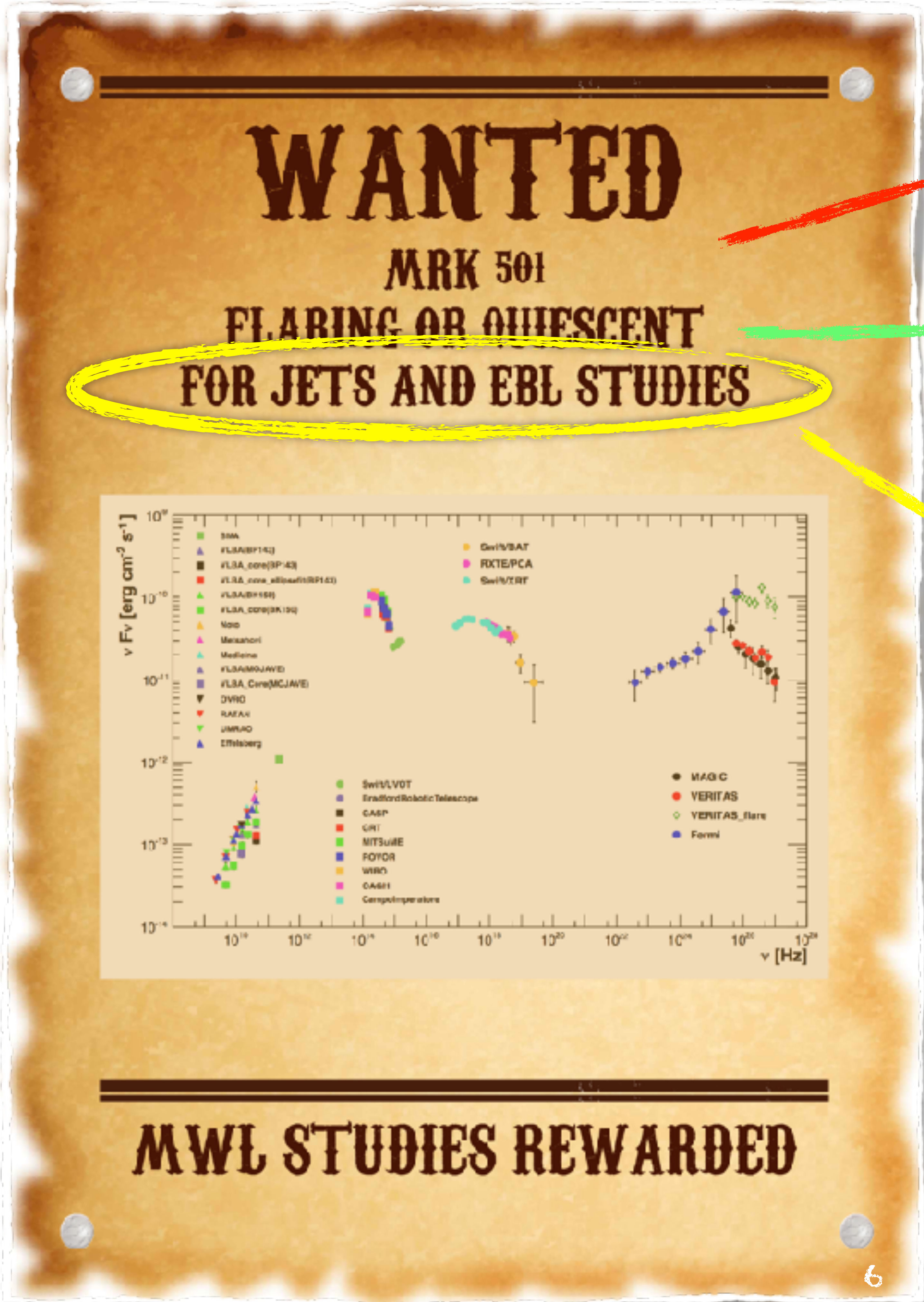

Mrk 501:

high-peaked BL Lac at z=0.03
a famous TeV emitter

Its persistent TeV emission during flaring and quiescent phases makes this blazar an excellent candidate for detailed multi-wavelength studies

Mrk 501 and Mrk 421 (the closest TeV blazar) have been detected up to few tens of TeV during extreme flares which allow us to probe the extragalactic background light (EBL) up to longer wavelengths than any other known TeV blazar

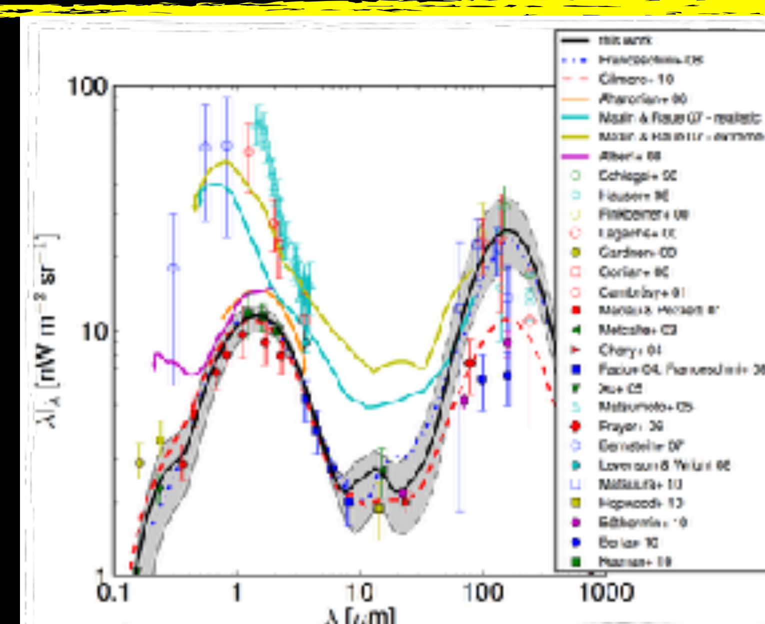

Extreme X-ray flaring activity in 2014

Outstanding X-ray activity during one of our MWL campaigns, in July 2014.

Largest X-ray flux detected by Neil Gehrels Swift-XRT in 13 years of operation.

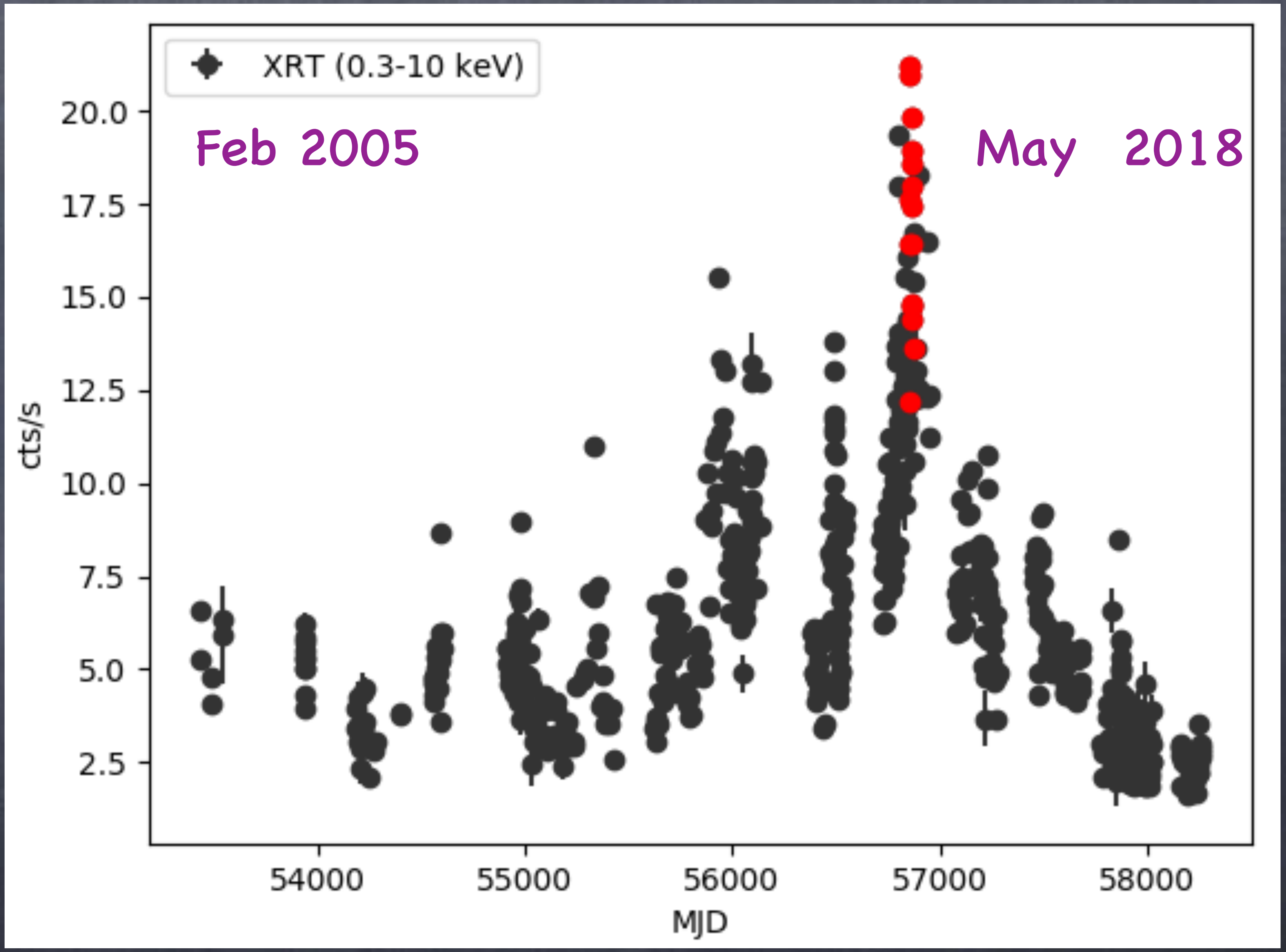

Extreme X-ray flaring activity in 2014

Outstanding X-ray activity during one of our MWL campaigns, in July 2014.

Largest X-ray flux detected by Neil Gehrels Swift-XRT in 13 years of operation.

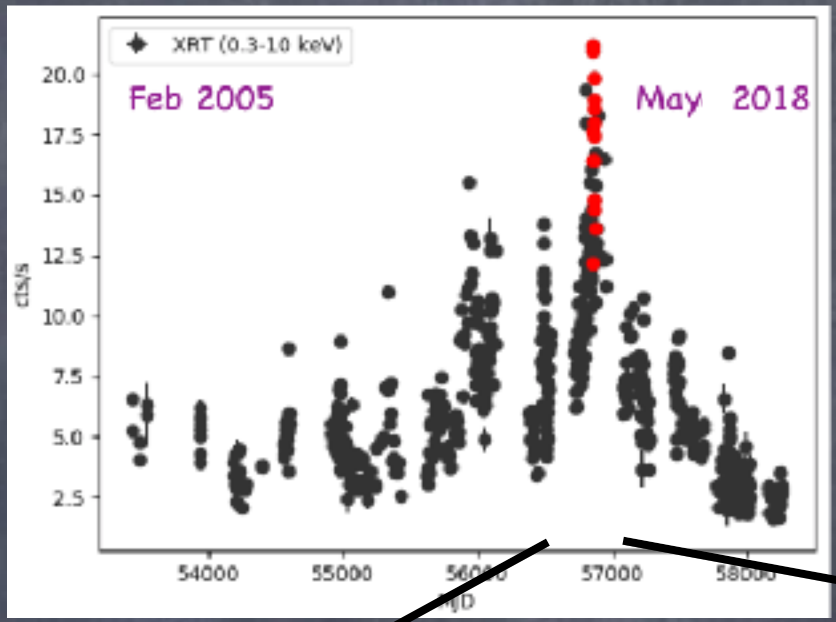

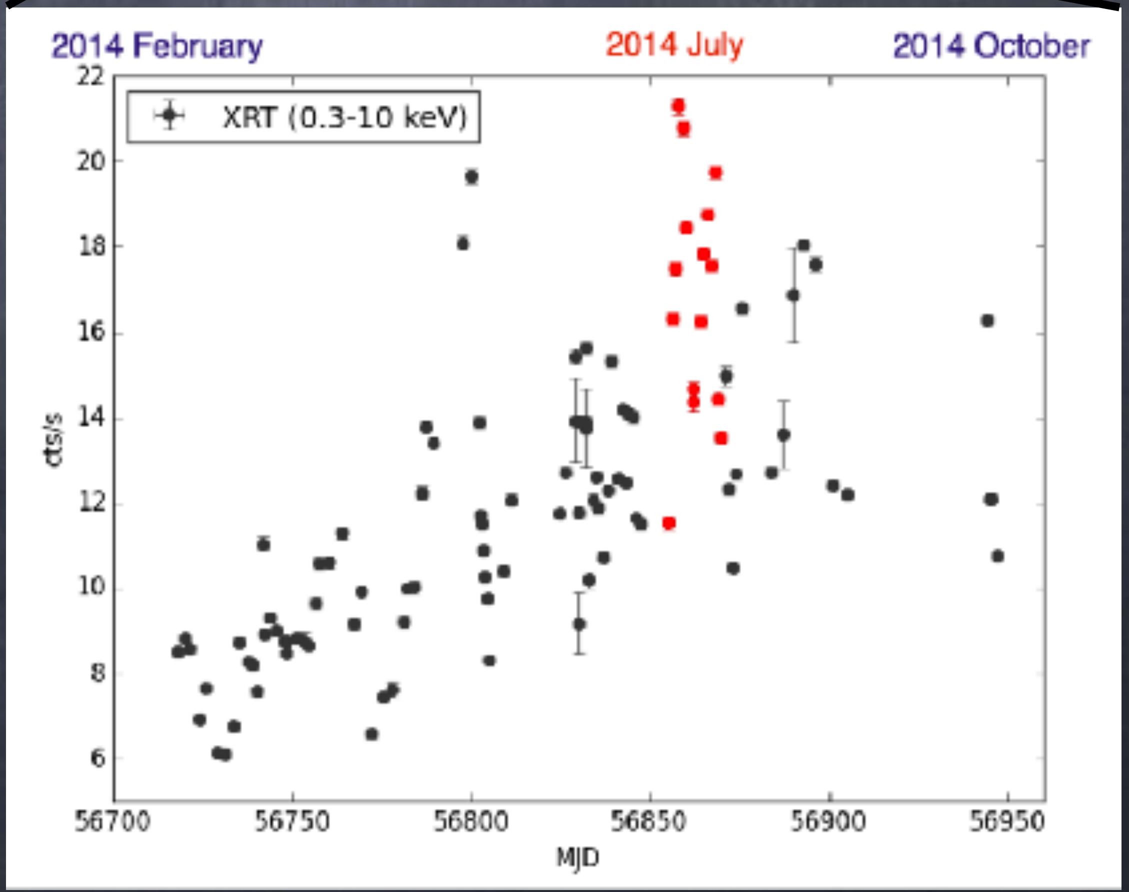

MWL flux evolution during the 2014 flare

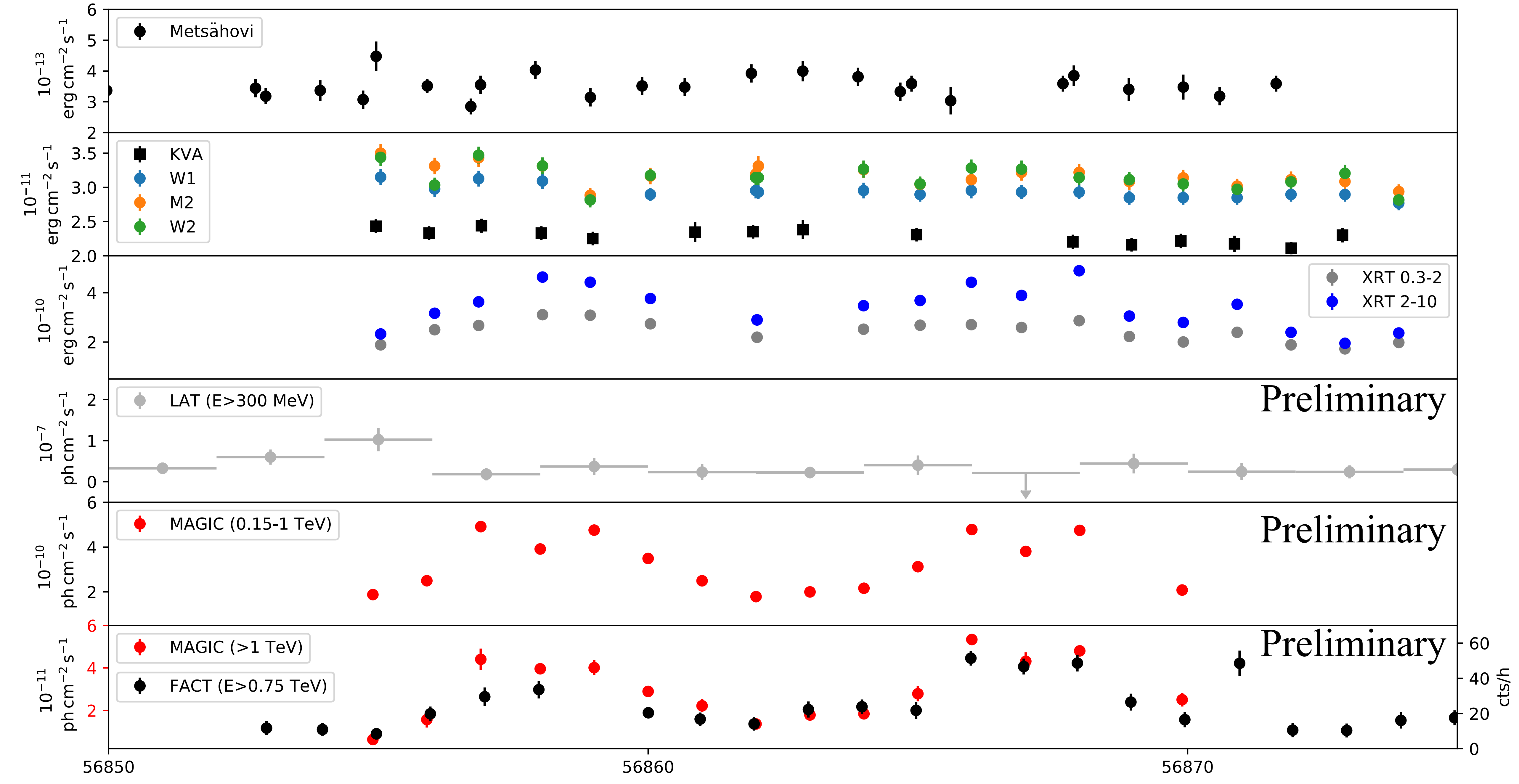

VHE vs X-ray correlations

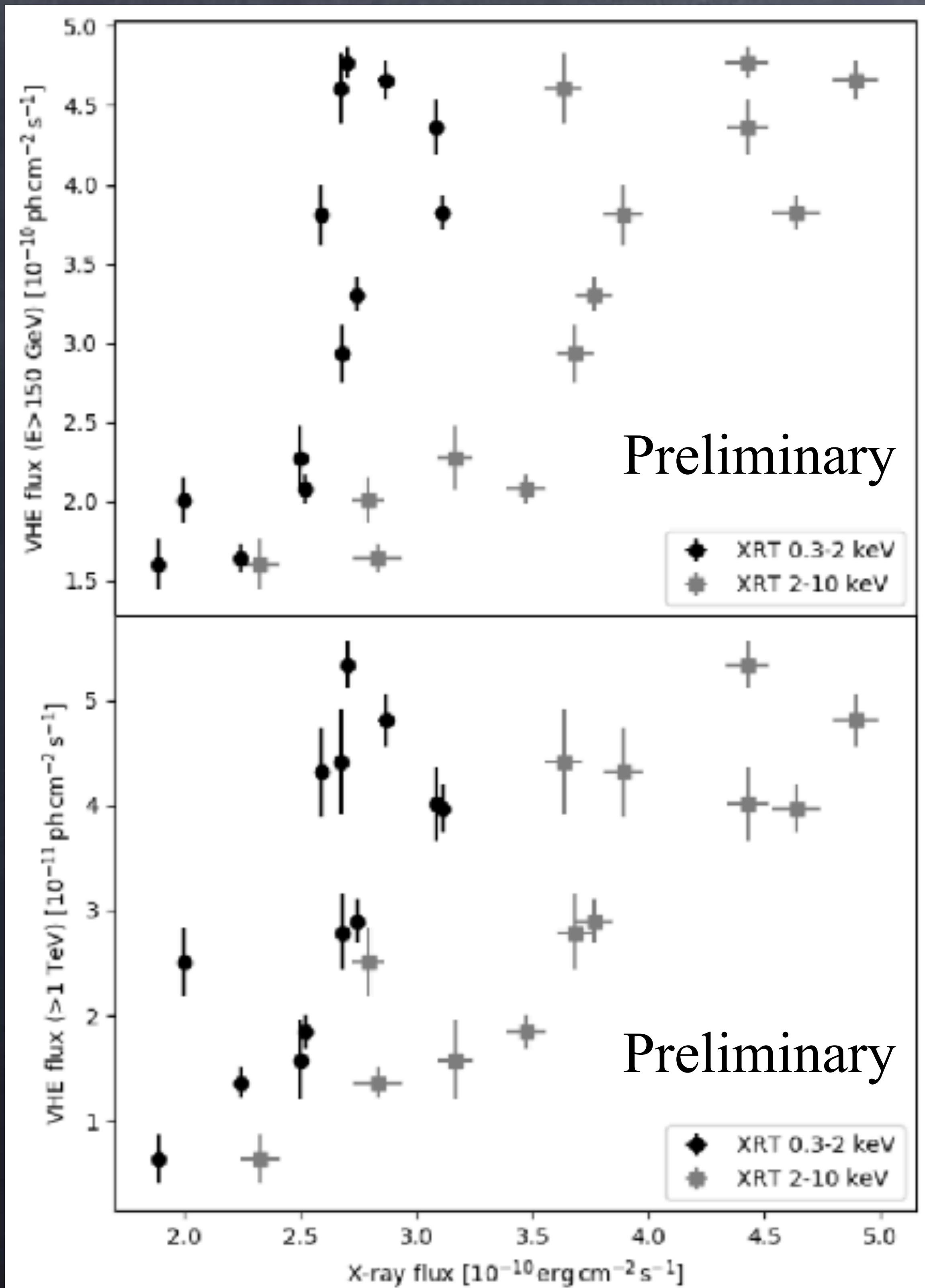

	VHE: 0.15-1 TeV	VHE: E>1 TeV
X-rays: 0.3-2 keV	0.73 (2.8σ) DCF=0.7+/-0.2	0.59(2.0σ) DCF=0.6+/-0.2
X-rays: 2-10 keV	0.85 (3.7σ) DCF=0.8+/-0.2	0.81(3.4σ) DCF=0.8+/-0.2

Hint of correlation between the VHE and the X-ray band

Fractional variability Mrk 501

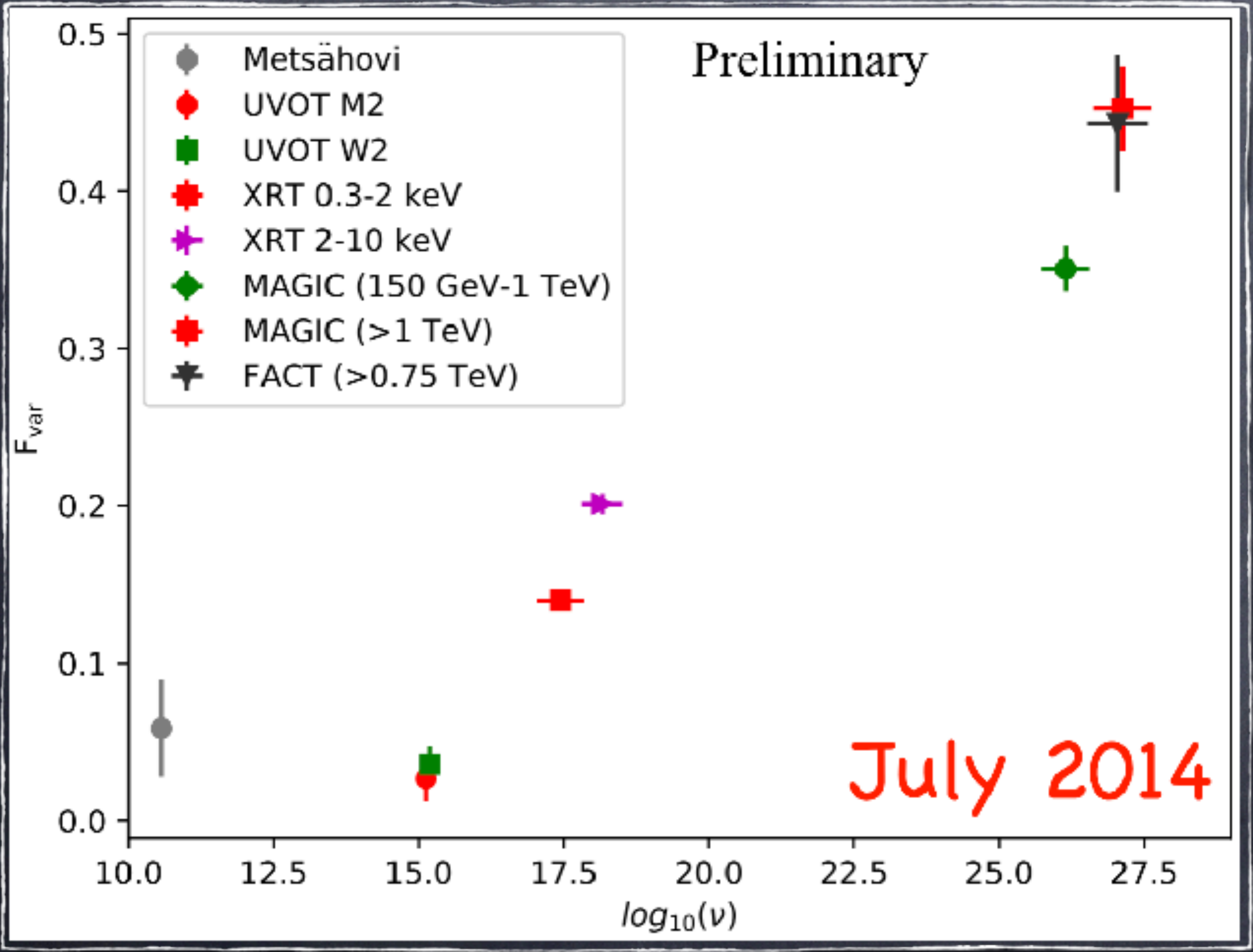

Variability quantified following prescription from Vaughan et al. 2003:

$$F_{var} = \sqrt{\frac{S - \langle \sigma_{err} \rangle^2}{\langle Flux \rangle^2}}$$

MWL SED overview

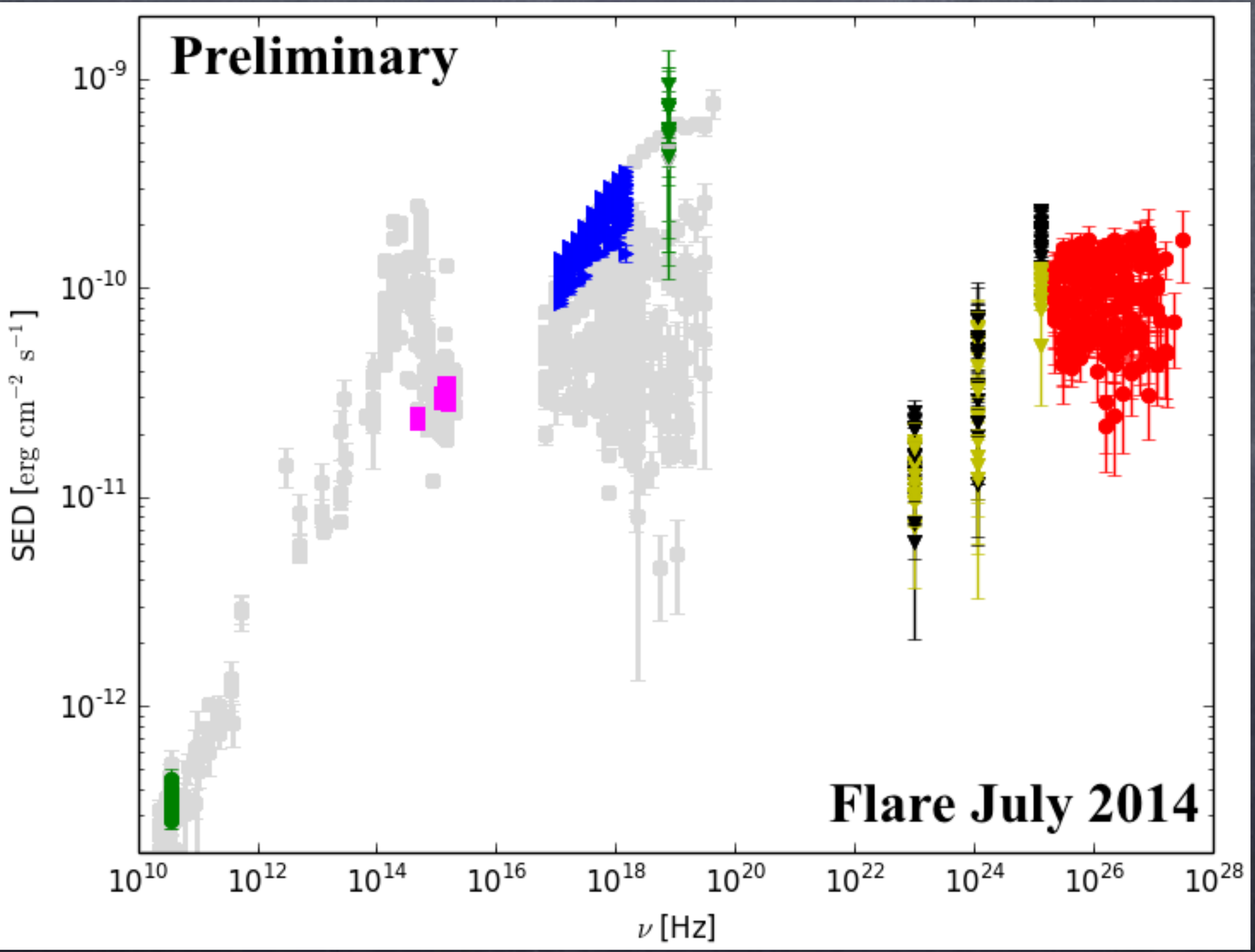

MWL SED overview

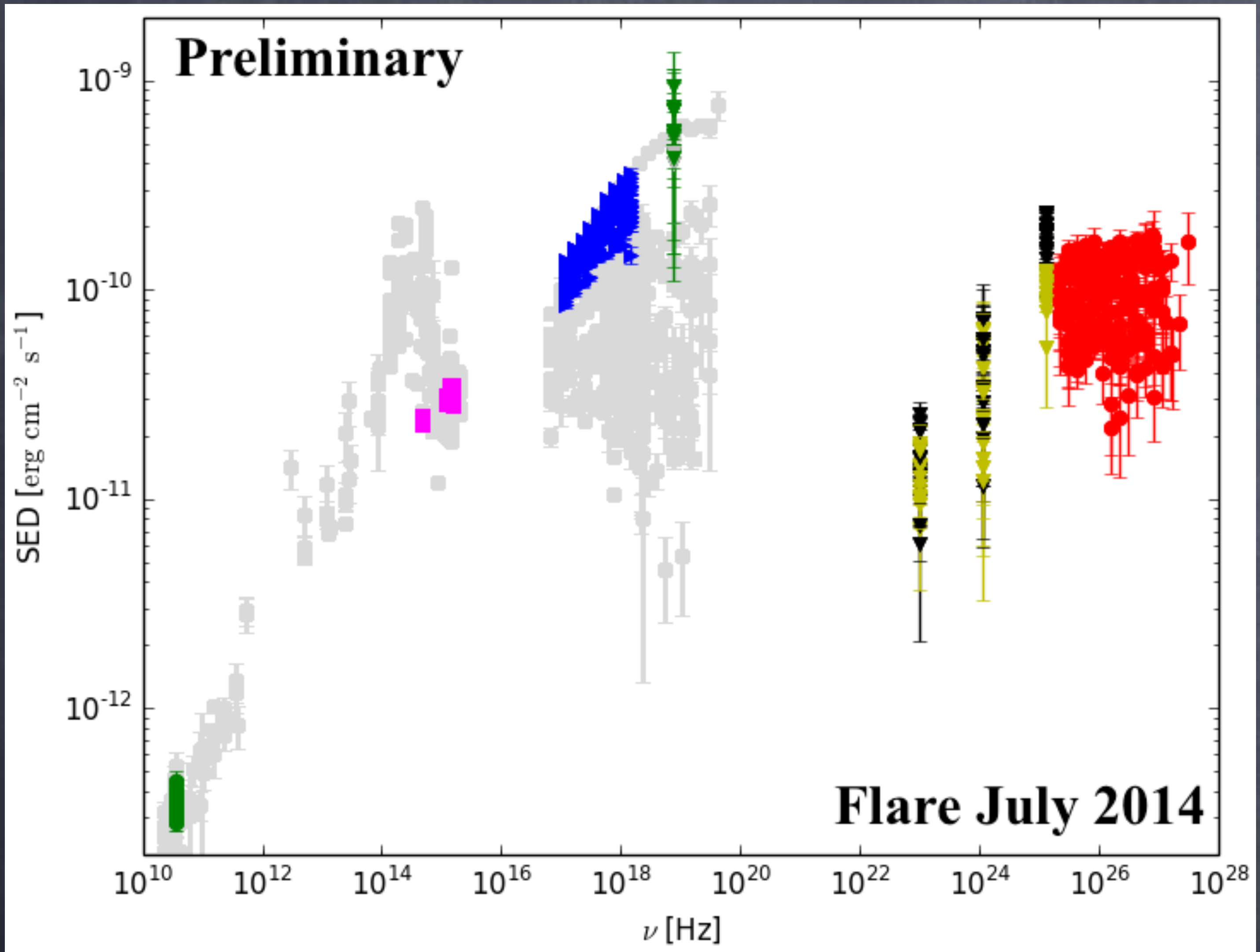

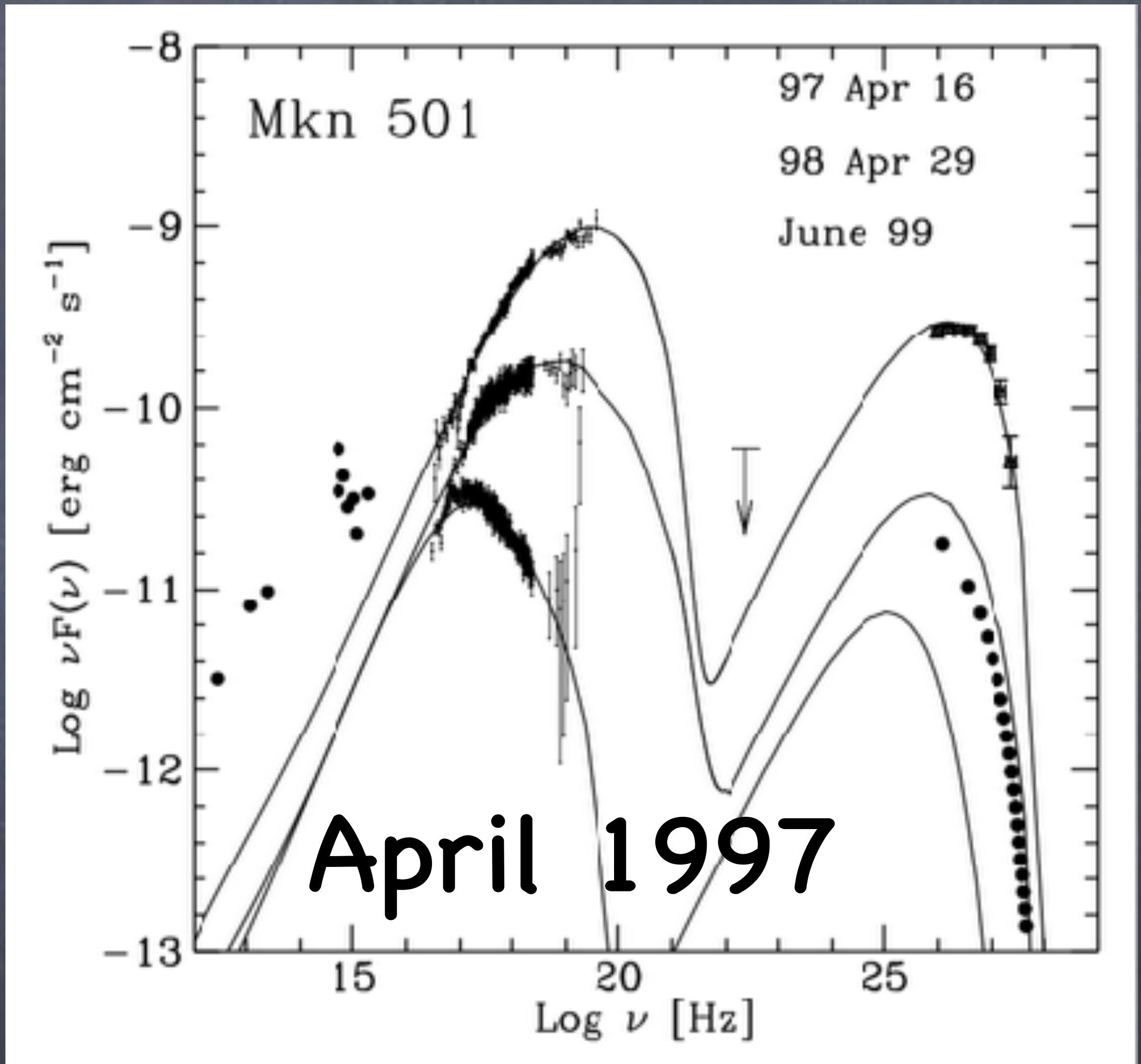

Tavecchio et al. (2001)
ApJ 554, 725

X-ray flux comparable
TeV more variable in 1997

Radio-optical correlation

- Lindfors et al. 2016 found a 2σ correlation hint between radio and optical from longterm light curves. It suggests that at least ~20% of the optical flux would originate from common radio-optical component.
- An extra large SSC component could explain the radio-optical emission.
- The jet from Mrk 501 is structured as revealed in radio wavelengths (Giroletti et al. 2004, 2008, Kojama et al. 2016). Therefore, this model might be too simple.

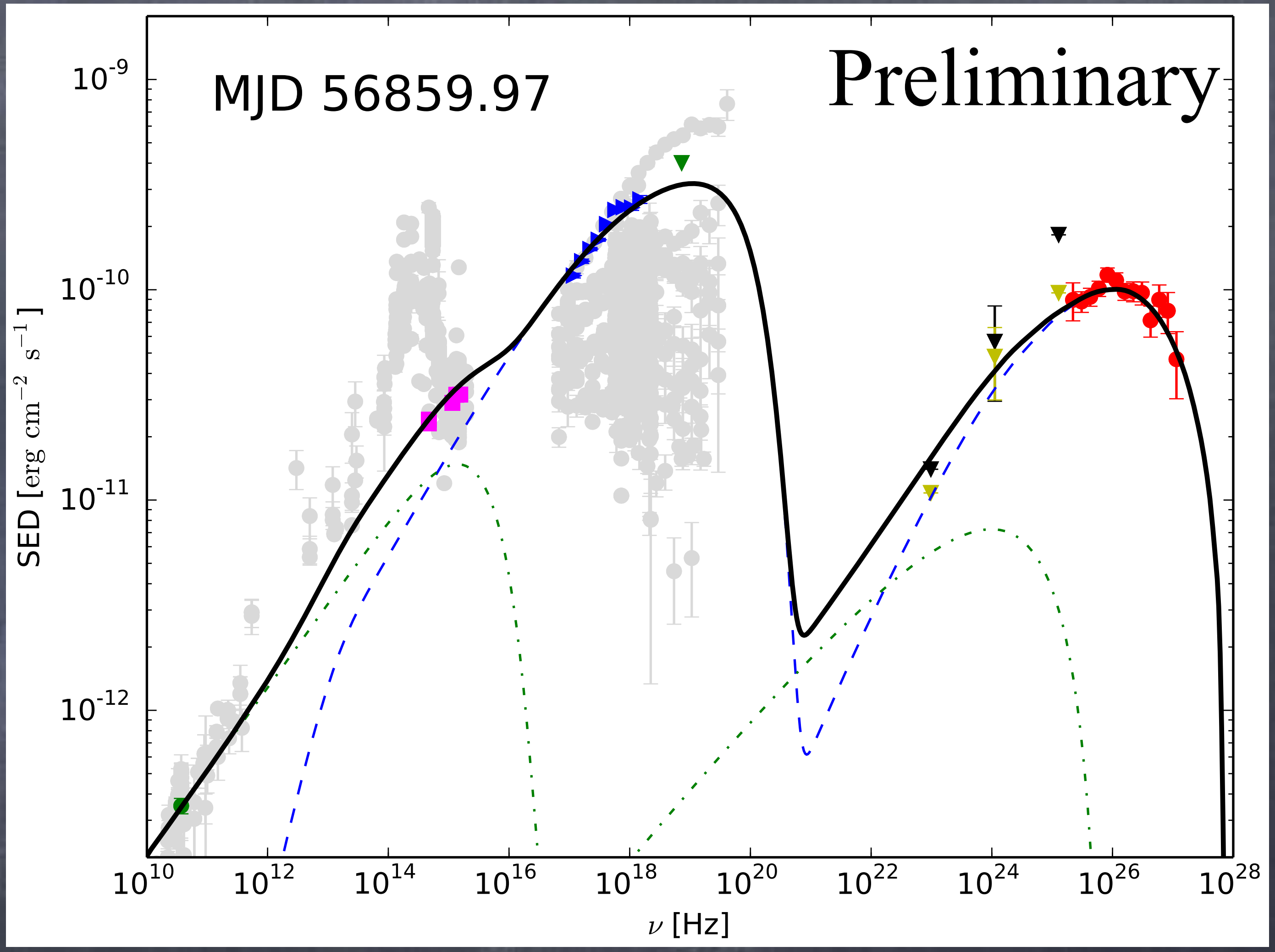

Synchrotron Self-Compton model

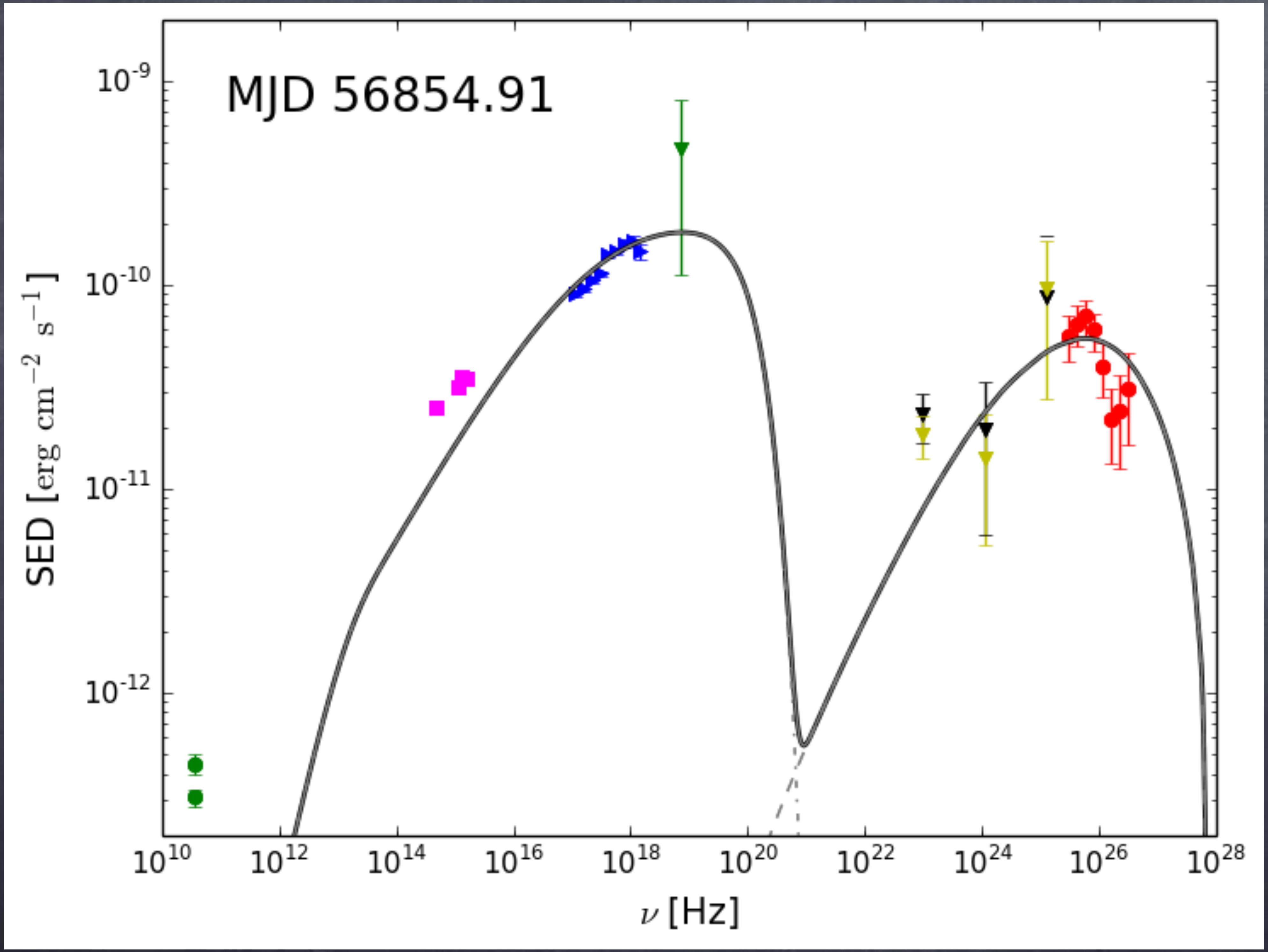

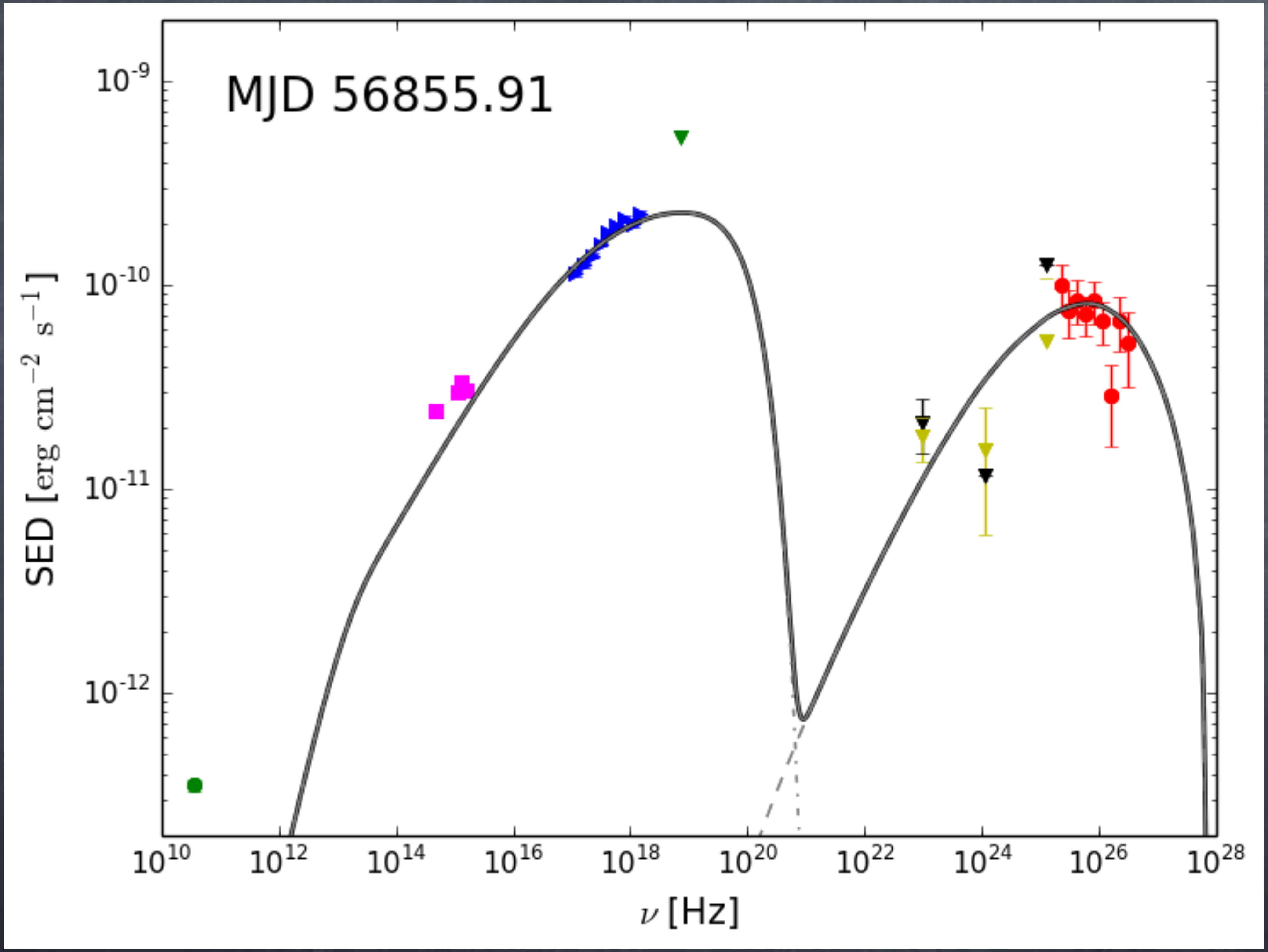

MJD 56855.91
SED [erg cm^{-2} s^{-1}]
ν [Hz]

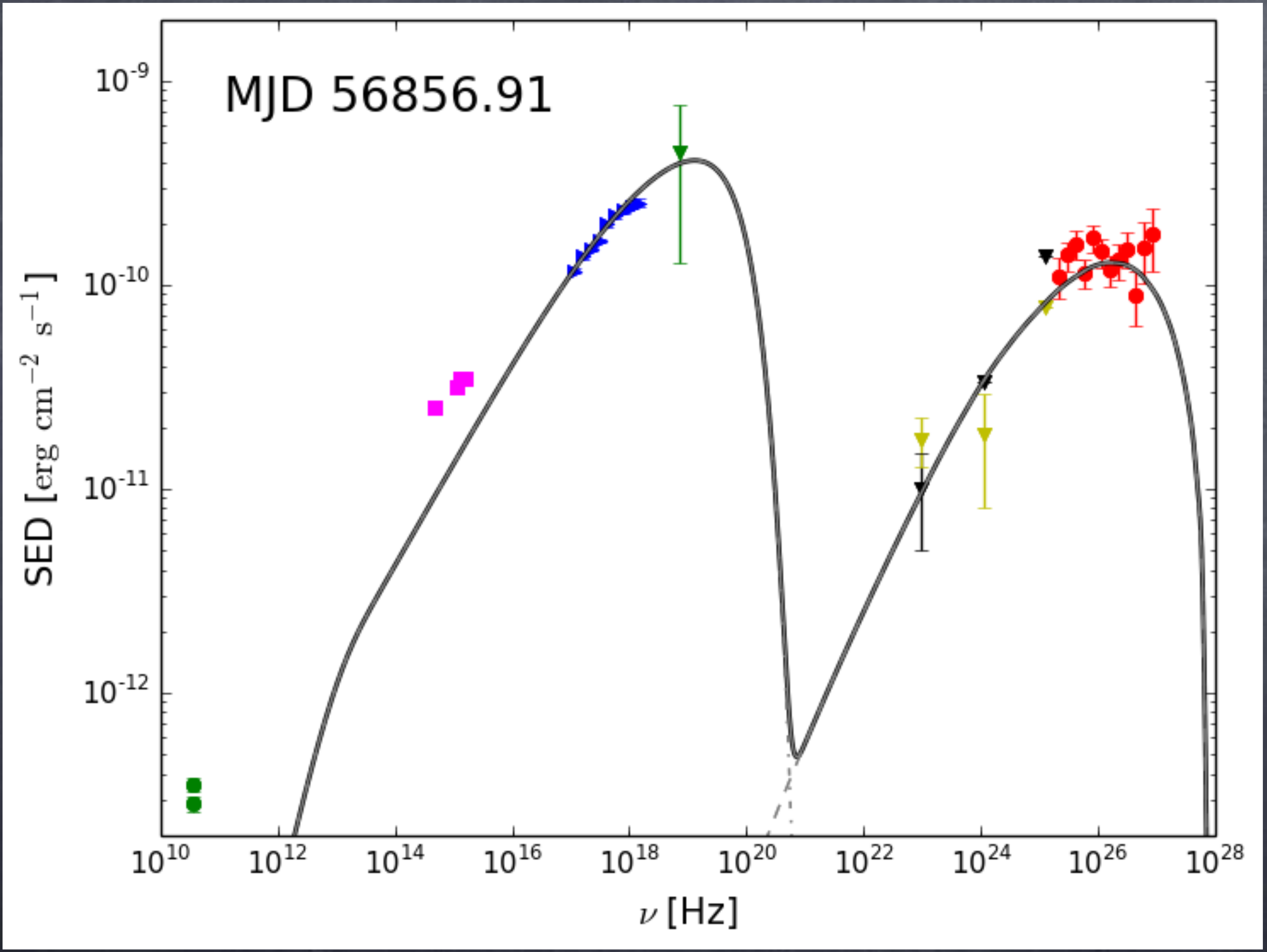
MJD 56856.91
SED [erg cm^{-2} s^{-1}]
ν [Hz]
10^{-9}
10^{-10}
10^{-11}
10^{-12}
10^{10}
10^{12}
10^{14}
10^{16}
10^{18}
10^{20}
10^{22}
10^{24}
10^{26}
10^{28}

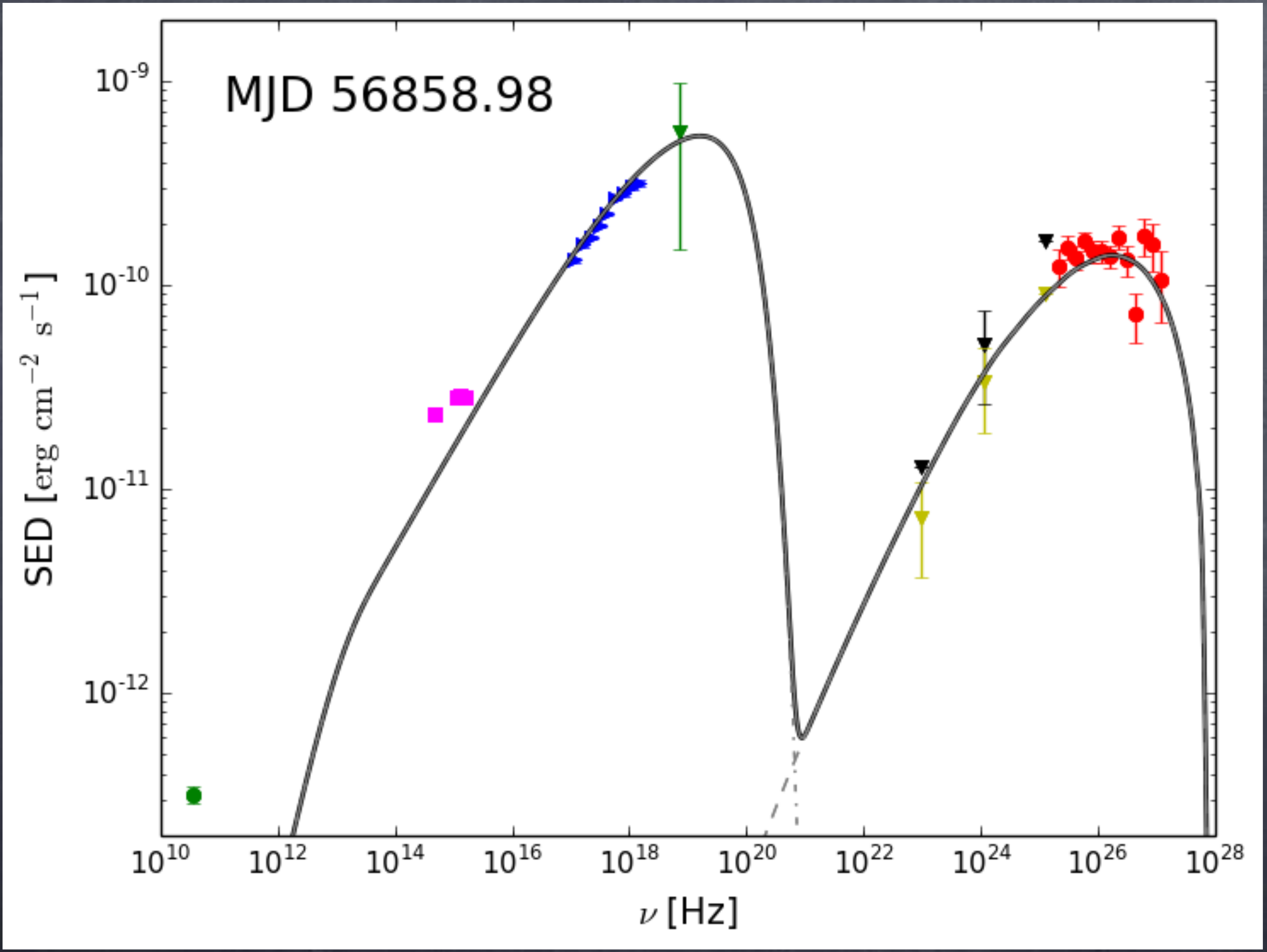
MJD 56858.98
SED [erg cm^{-2} s^{-1}]
10^{-9}
10^{-10}
10^{-11}
10^{-12}
10^{10}
10^{12}
10^{14}
10^{16}
10^{18}
10^{20}
10^{22}
10^{24}
10^{26}
10^{28}
ν [Hz]

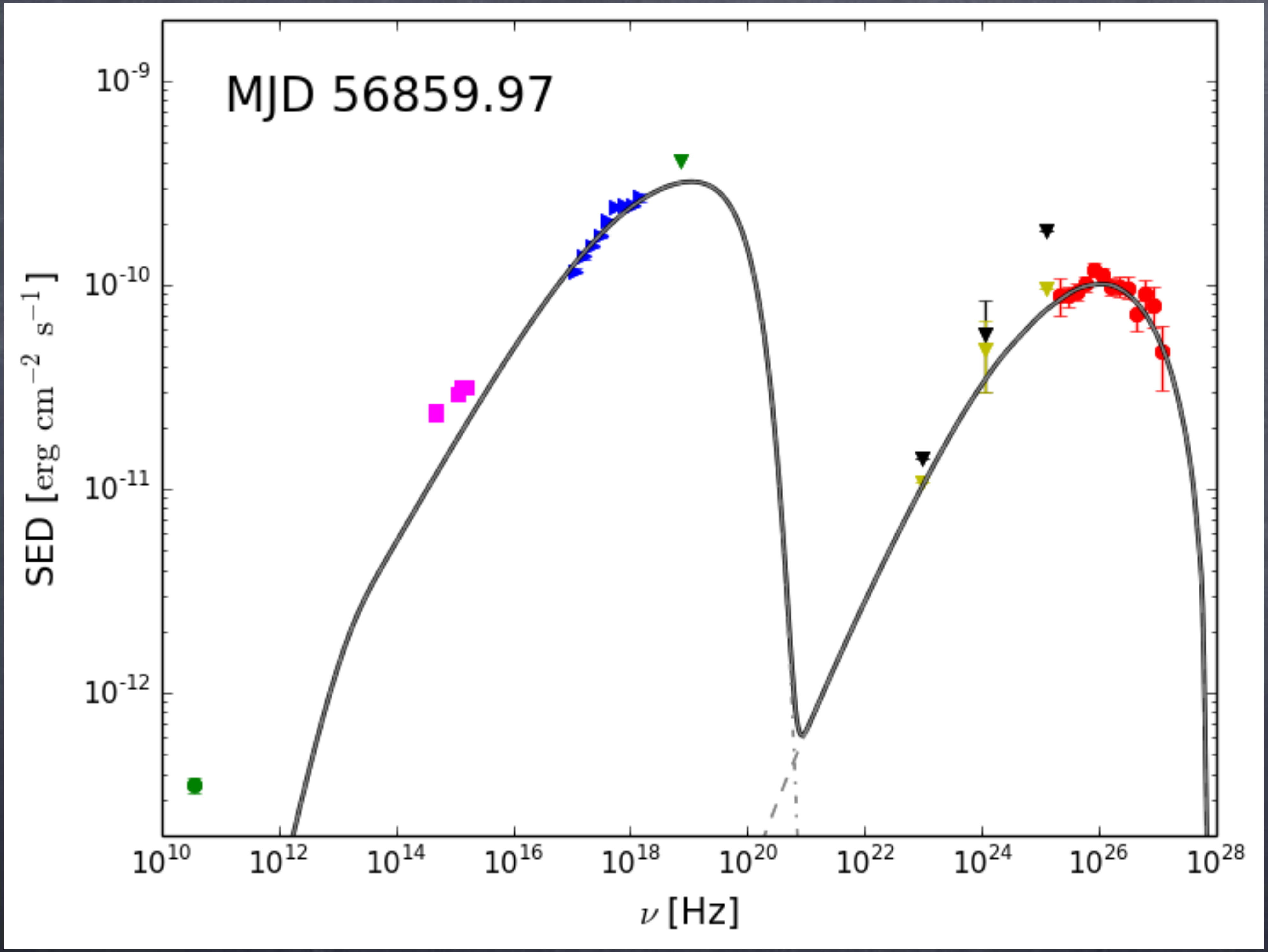

MJD 56859.97
SED [erg cm^{-2} s^{-1}]
10^{-9}
10^{-10}
10^{-11}
10^{-12}
10^{10}
10^{12}
10^{14}
10^{16}
10^{18}
10^{20}
10^{22}
10^{24}
10^{26}
10^{28}
ν [Hz]

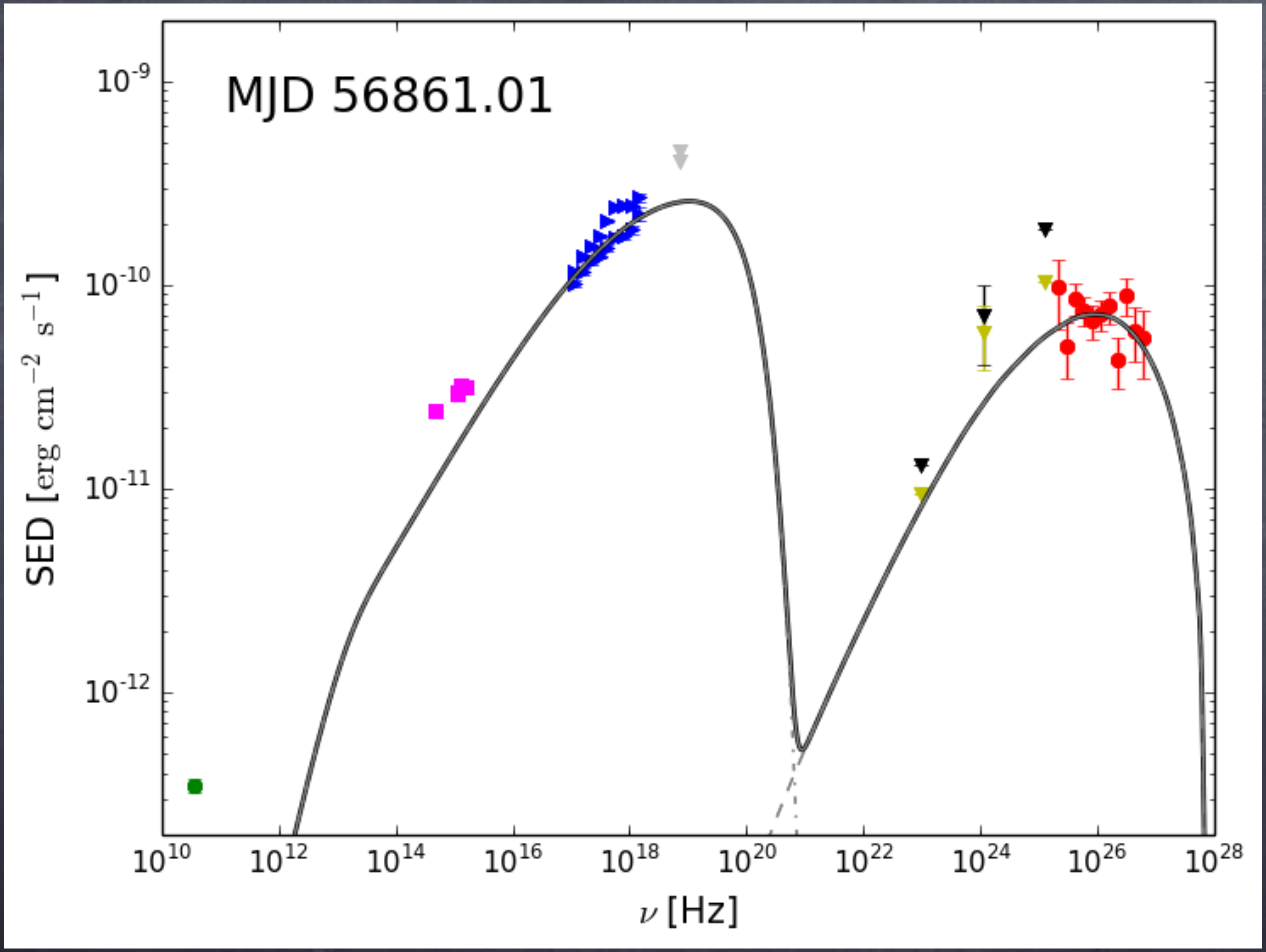
MJD 56861.01
SED [erg cm^{-2} s^{-1}]
10^{-9}
10^{-10}
10^{-11}
10^{-12}
10^{10} 10^{12} 10^{14} 10^{16} 10^{18} 10^{20} 10^{22} 10^{24} 10^{26} 10^{28}
ν [Hz]

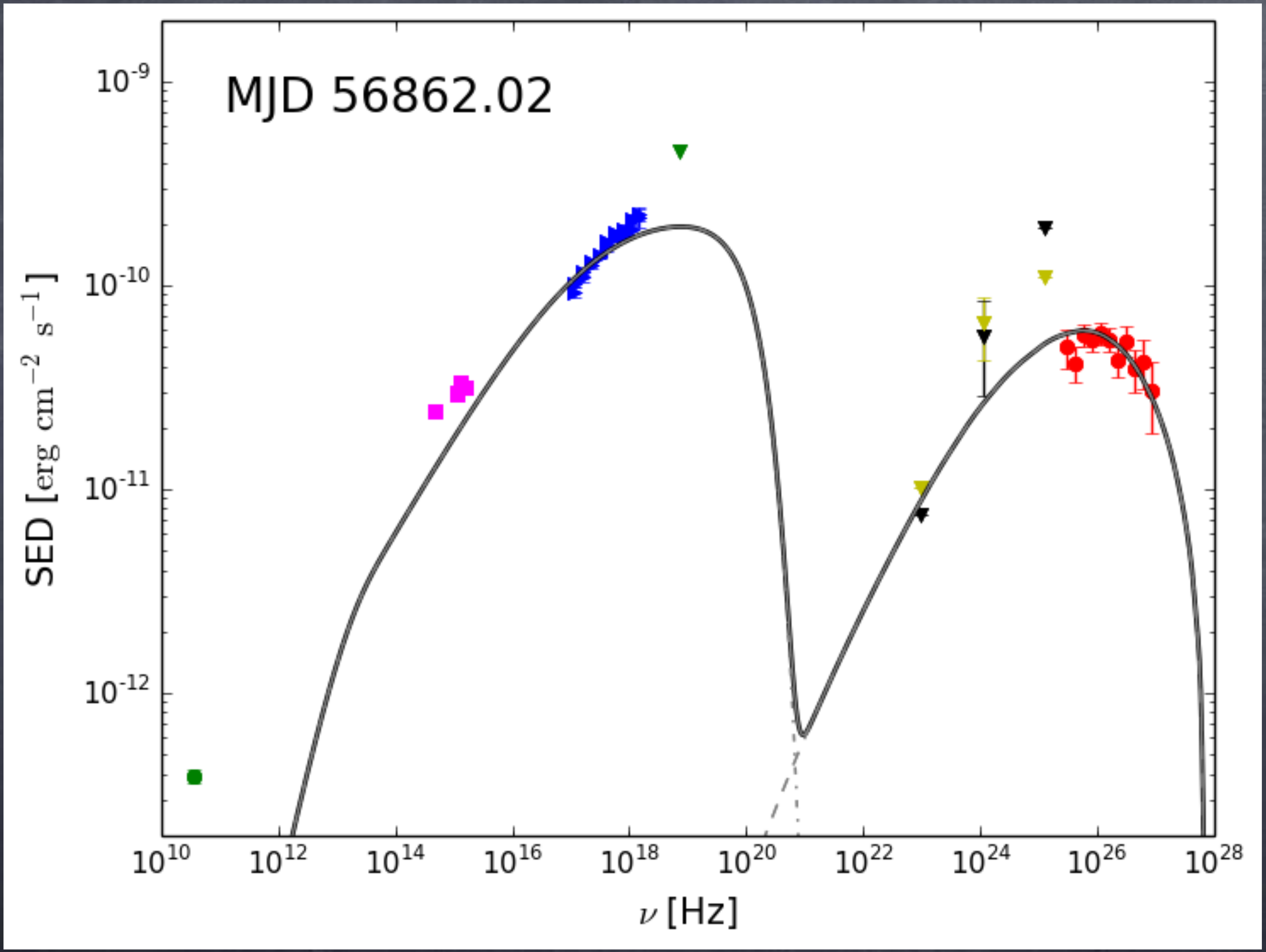
MJD 56862.02
SED [erg cm^{-2} s^{-1}]
10^{-9}
10^{-10}
10^{-11}
10^{-12}
10^{10}
10^{12}
10^{14}
10^{16}
10^{18}
10^{20}
10^{22}
10^{24}
10^{26}
10^{28}
ν [Hz]

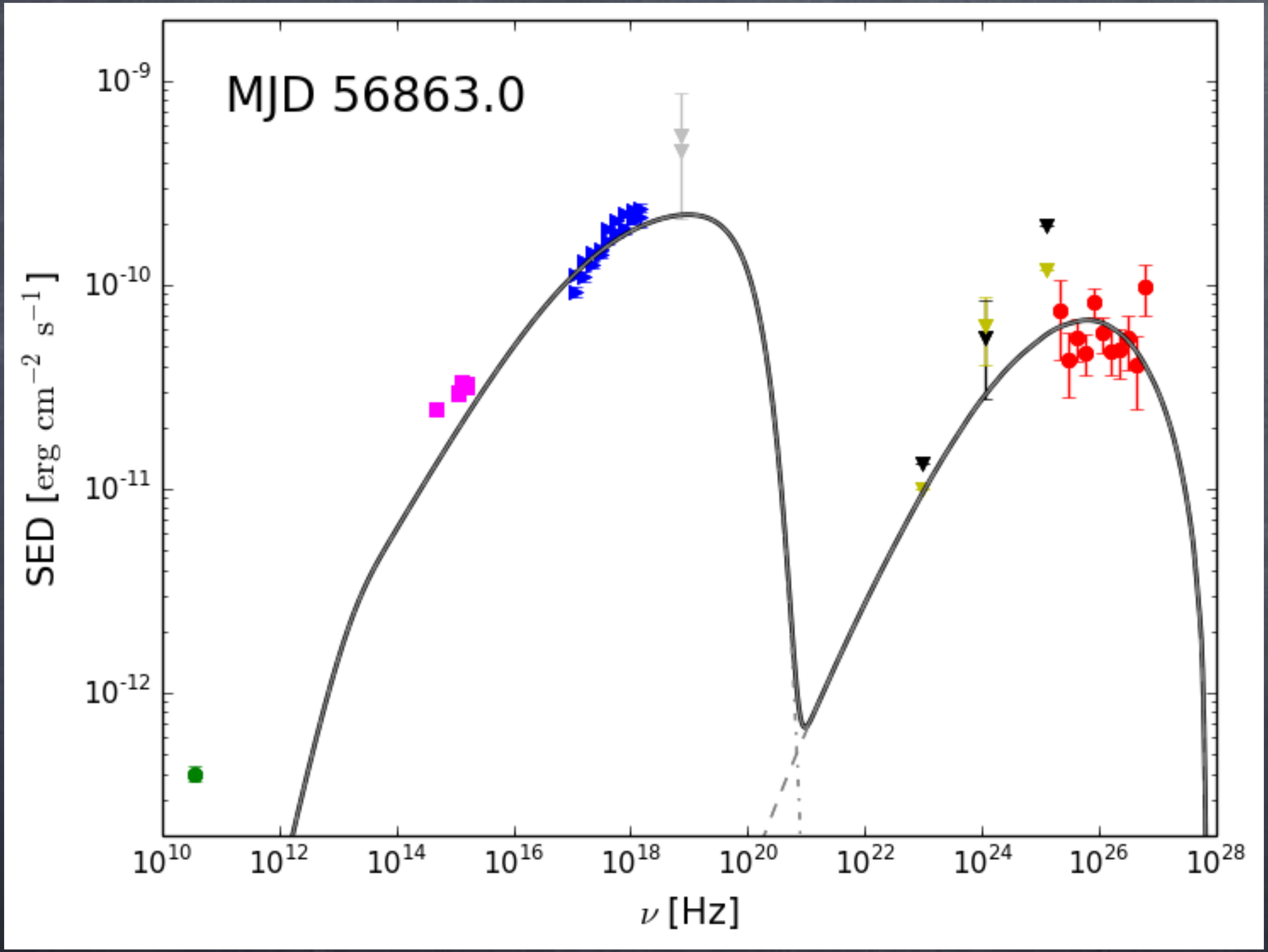

MJD 56863.0
SED [erg cm^{-2} s^{-1}]
10^{-9}
10^{-10}
10^{-11}
10^{-12}
10^{10}
10^{12}
10^{14}
10^{16}
10^{18}
10^{20}
10^{22}
10^{24}
10^{26}
10^{28}
ν [Hz]

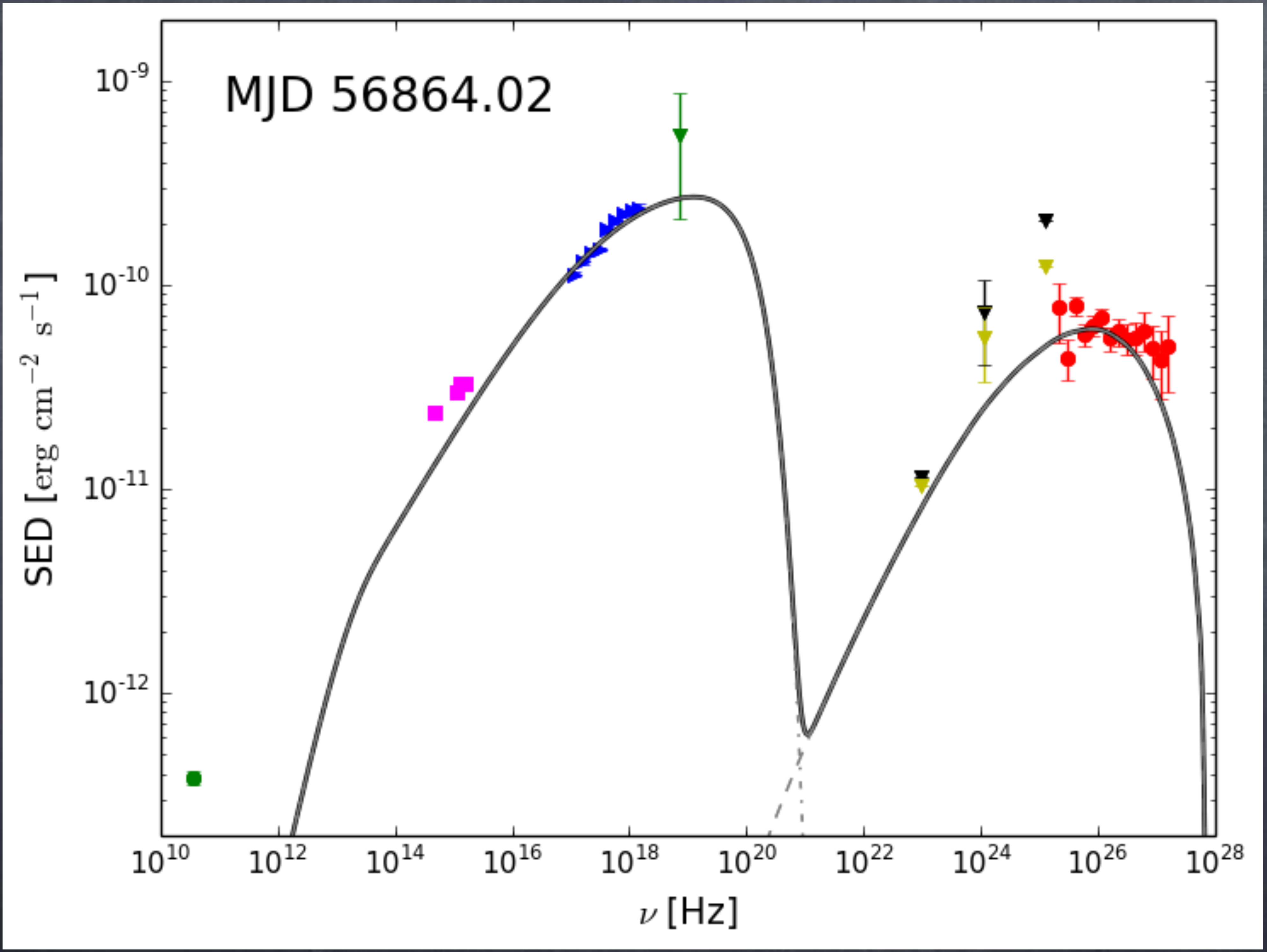
MJD 56864.02
SED [erg cm^{-2} s^{-1}]
ν [Hz]
10^{-9}
10^{-10}
10^{-11}
10^{-12}
10^{10}
10^{12}
10^{14}
10^{16}
10^{18}
10^{20}
10^{22}
10^{24}
10^{26}
10^{28}

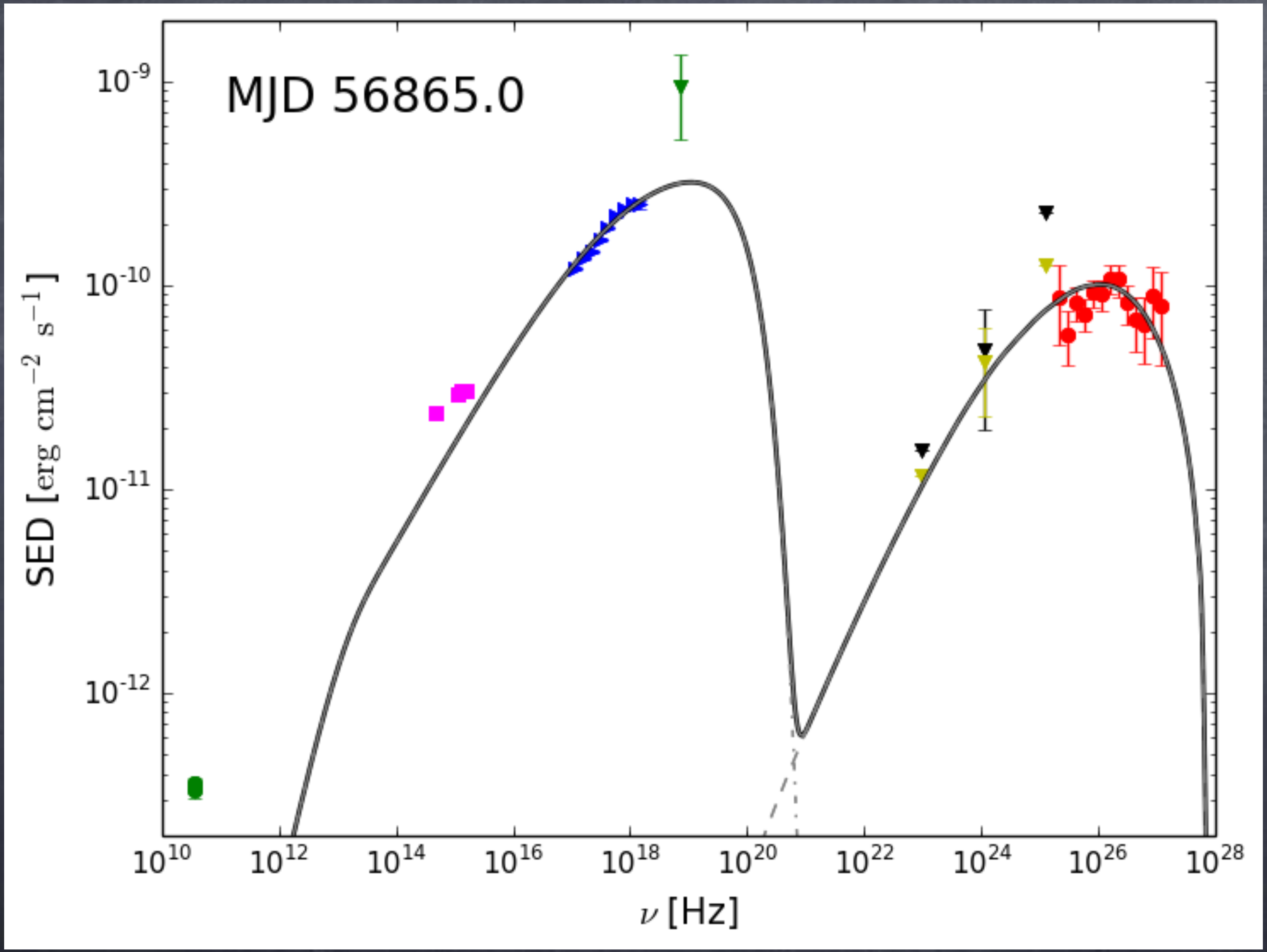
MJD 56865.0
SED [erg cm^{-2} s^{-1}]
ν [Hz]
10^{-9}
10^{-10}
10^{-11}
10^{-12}
10^{10} 10^{12} 10^{14} 10^{16} 10^{18} 10^{20} 10^{22} 10^{24} 10^{26} 10^{28}

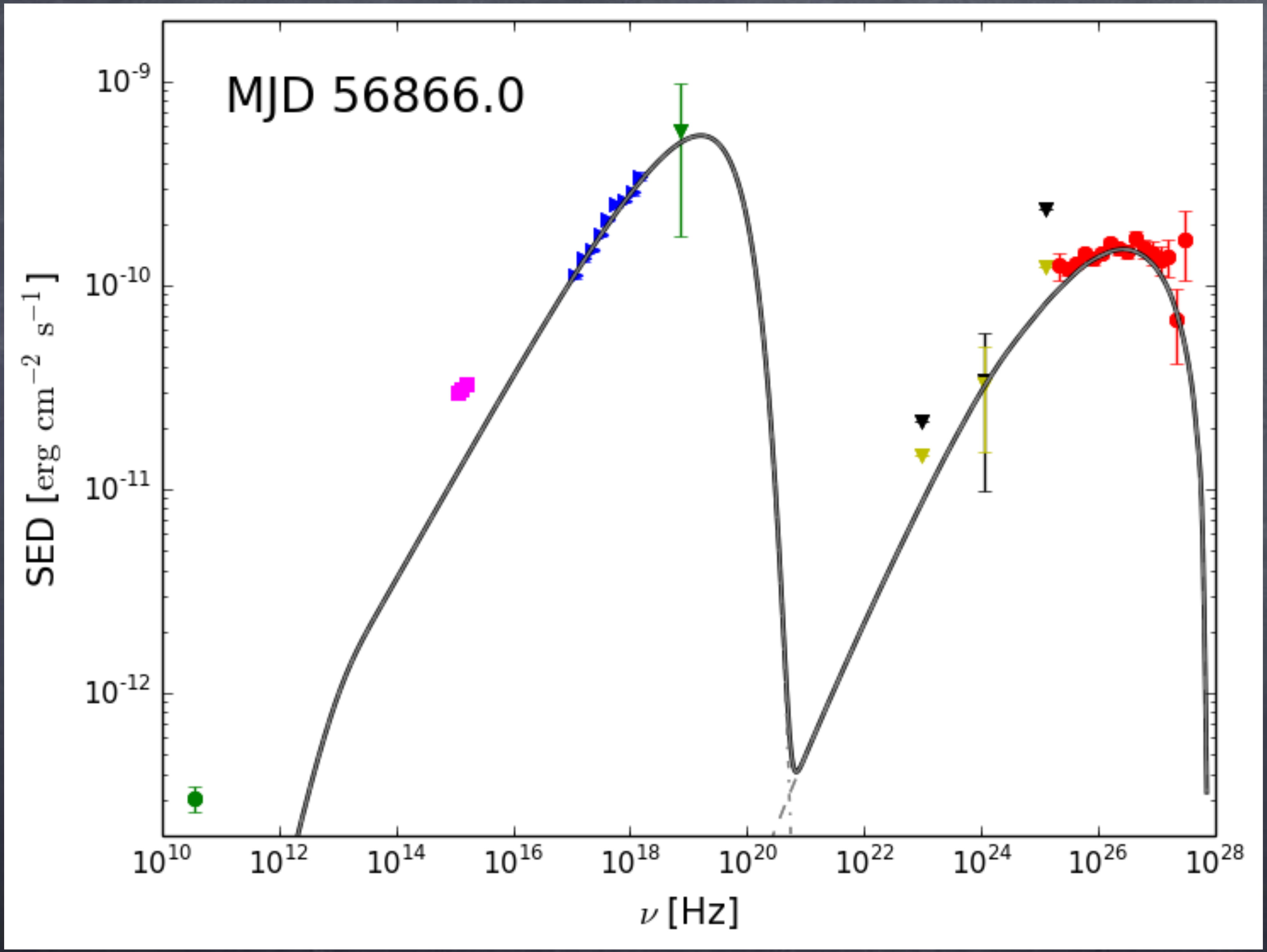
MJD 56866.0
SED [erg cm^{-2} s^{-1}]
ν [Hz]
10^{-9}
10^{-10}
10^{-11}
10^{-12}
10^{10}
10^{12}
10^{14}
10^{16}
10^{18}
10^{20}
10^{22}
10^{24}
10^{26}
10^{28}

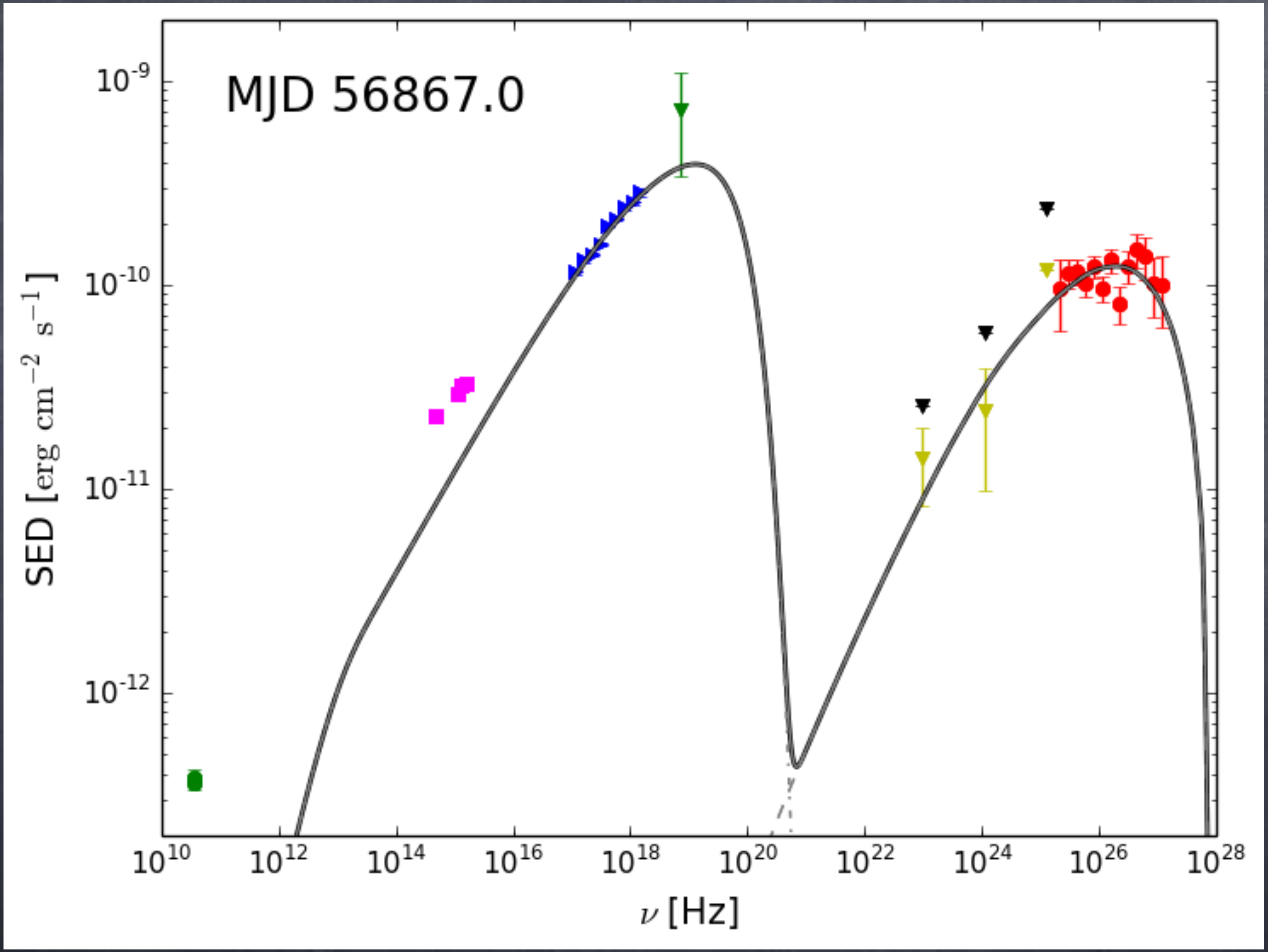
MJD 56867.0
SED [erg cm^{-2} s^{-1}]
10^{-9}
10^{-10}
10^{-11}
10^{-12}
10^{10}
10^{12}
10^{14}
10^{16}
10^{18}
10^{20}
10^{22}
10^{24}
10^{26}
10^{28}
ν [Hz]

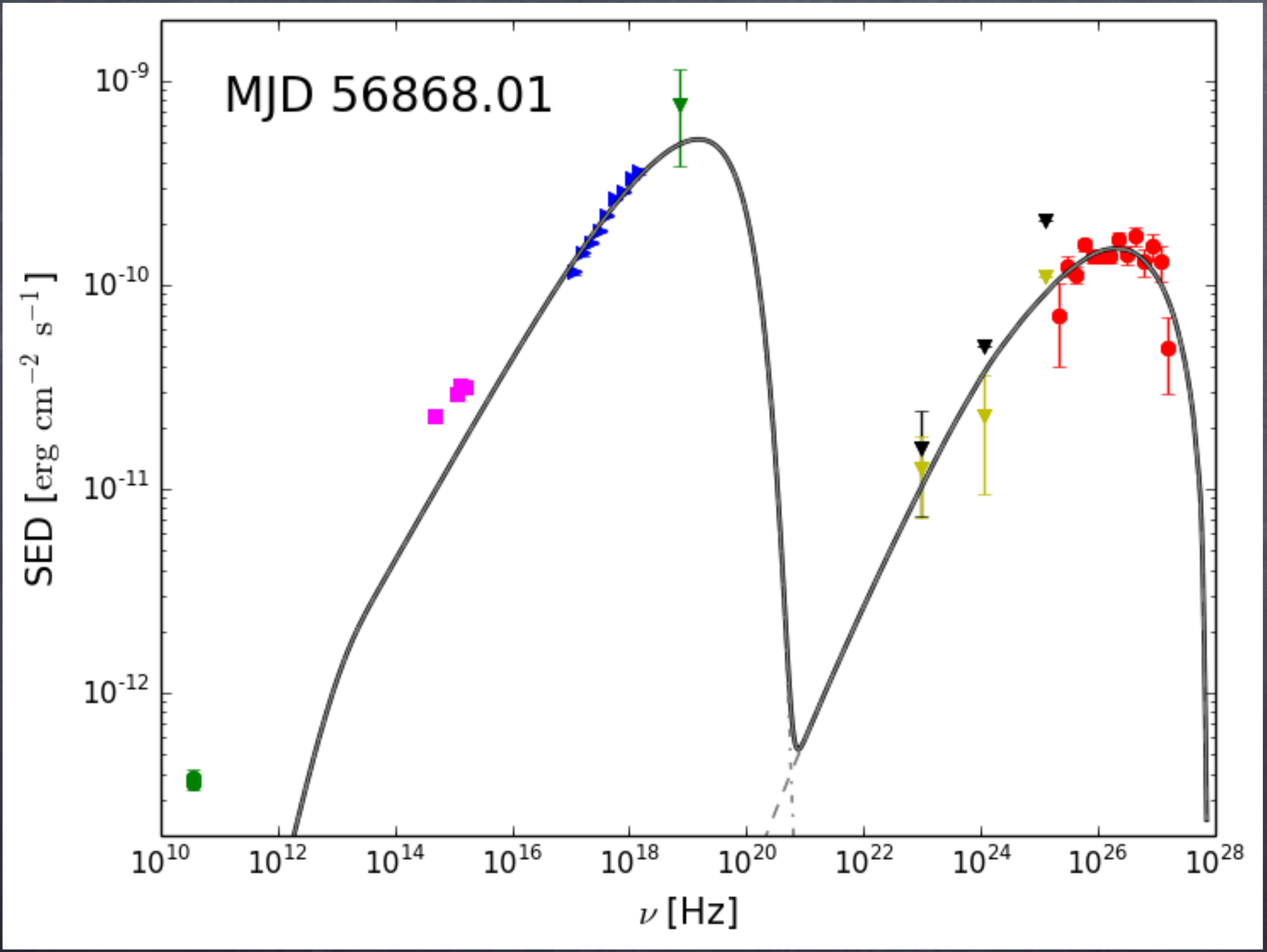
MJD 56868.01
SED [erg cm^{-2} s^{-1}]
ν [Hz]
10^{-9}
10^{-10}
10^{-11}
10^{-12}
10^{10}
10^{12}
10^{14}
10^{16}
10^{18}
10^{20}
10^{22}
10^{24}
10^{26}
10^{28}

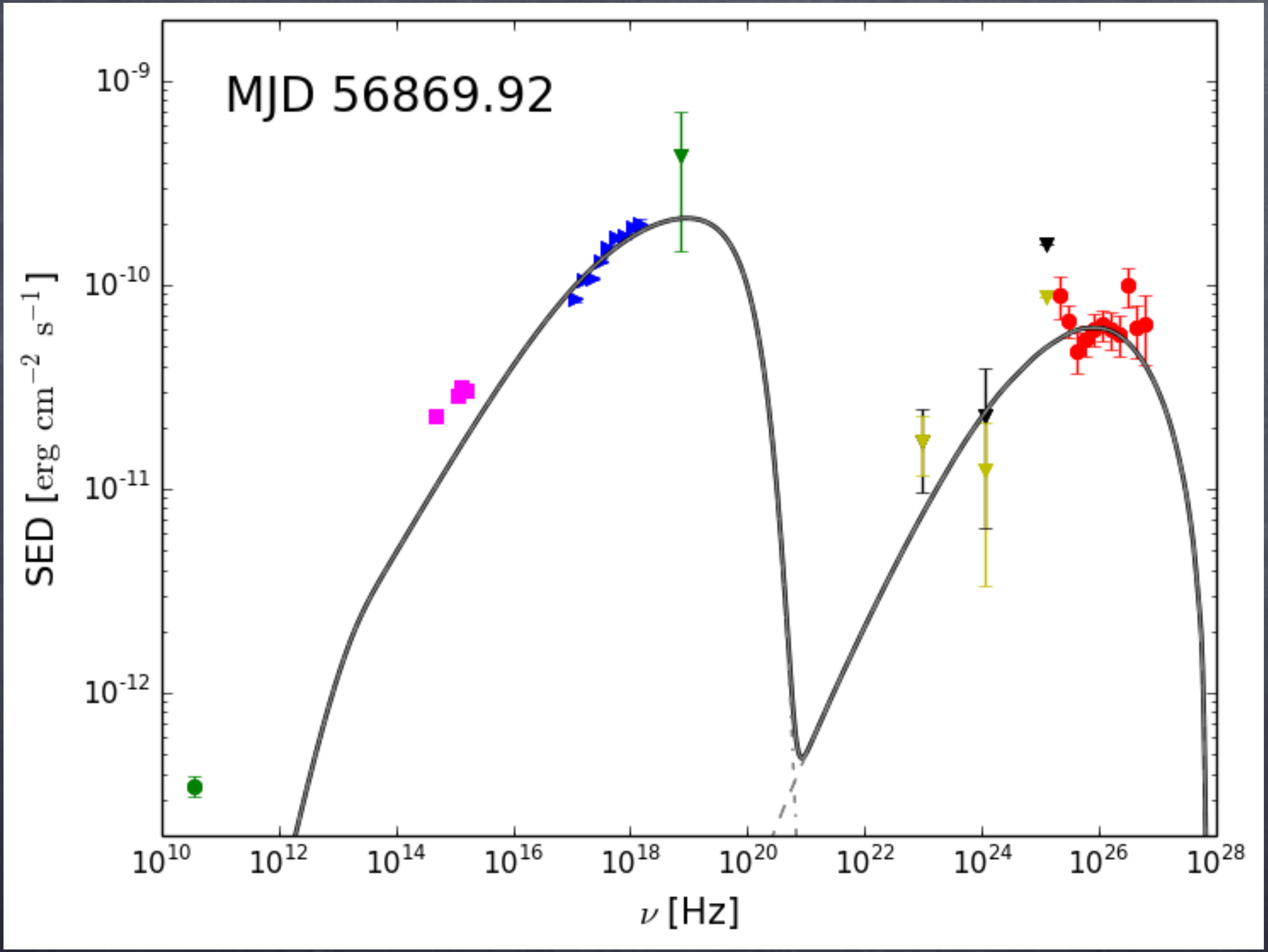
MJD 56869.92
SED [erg cm^{-2} s^{-1}]
ν [Hz]
10^{-9}
10^{-10}
10^{-11}
10^{-12}
10^{10} 10^{12} 10^{14} 10^{16} 10^{18} 10^{20} 10^{22} 10^{24} 10^{26} 10^{28}

SSC parameters

$\gamma min = 10^3$

$\gamma max = 3\times10^6$

density $= 2.1\times10^4$ cm^{-3}

R $= 2.7\times10^{15}$ cm

$\delta = 20$

MJD	γ_b [10^5]	n1	n2	B [G]
56854.91	2.0	2.018	3.1	0.125
56855.91	2.0	2.00	3.1	0.125
56856.91	8.5	1.99	3.1	0.087
56857.98	4.0	2.00	3.1	0.12
56858.98	9.0	2.00	3.1	0.105
56859.97	4.0	2.00	3.1	0.11
56861.01	3.5	2.015	3.1	0.115
56862.02	1.9	2.015	3.1	0.13
56863.00	1.9	2.01	3.05	0.13
56864.02	2.5	2.03	3.05	0.145
56865.00	4.0	2.00	3.1	0.11
56866.00	20.0	1.99	3.1	0.078
56867.00	9.5	1.99	3.1	0.082
56868.01	11.0	1.99	3.1	0.09
56869.92	3.0	2.016	3.1	0.112

Preliminary

SSC parameters

$\gamma min = 10^3$

$\gamma max = 3 \times 10^6$

$\text{density} = 2.1 \times 10^4\ \text{cm}^{-3}$

$R = 2.7 \times 10^{15}$ cm

$\delta = 20$

The 2-week flare can be explained with the evolution of the electron distribution energy break and the magnetic field

MJD	γ_b [10^5]	n1	n2	B [G]
56854.91	2.0	2.018	3.1	0.125
56855.91	2.0	2.00	3.1	0.125
56856.91	8.5	1.99	3.1	0.087
56857.98	4.0	2.00	3.1	0.12
56858.98	9.0	2.00	3.1	0.105
56859.97	4.0	2.00	3.1	0.11
56861.01	3.5	2.015	3.1	0.115
56862.02	1.9	2.015	3.1	0.13
56863.00	1.9	2.01	3.05	0.13
56864.02	2.5	2.03	3.05	0.145
56865.00	4.0	2.00	3.1	0.11
56866.00	20.0	1.99	3.1	0.078
56867.00	9.5	1.99	3.1	0.082
56868.01	11.0	1.99	3.1	0.09
56869.92	3.0	2.016	3.1	0.112

Preliminary

Take home message

- Detection of the historical maximum of the X-ray emission during the 13 years Swift-XRT operation (at the level of the historical 1997 flare)
- The multi-wavelength SED evolution during the flare can be explained mostly as changes in the energy break of the electrons and the magnetic field.

Thanks!